identified and quantified. These results demonstrate that AAA is a feasible method for biological significant proteins.

Experimental section

Reagents

BSA (A7638) and TG from bovine thyroid (T1001) were purchased from Sigma (St. Louis, MO). Sample solutions of BSA or TG were prepared on the basis of the dry weight of the proteins. HCl, sodium tetraborate, Coomassie brilliant blue (CBB) R-250, and tetrabutylammonium bromide (TBA-Br) were purchased from Wako (Osaka, Japan). A type H amino acid standard containing 17 amino acids (2.5 mmol/l each) was purchased from Pierce Chemical Co. (Rockford, IL), and LC/MS-grade acetonitrile (AN, A955-212) was purchased from Thermo Fisher Scientific Inc. (Waltham, MA). The phosphate buffer for chromatography was made from sodium dihydrogen phosphate monohydrate ($NaH_2PO_4 \cdot H_2O$, 106,346), and disodium hydrogen phosphate dihydrate ($Na_2HPO_4 \cdot 2H_2O$, 106,580) was purchased from Merck KGaA (Darmstadt, Germany). 3-cyclohexylamino-1-propanesulfonic acid (CAPS) was purchased from Nacalai Tesque, Inc. (Kyoto, Japan).

Amino acids were analyzed after pre-column derivatization with a fluorophore. The derivatization regent, AQC, was synthesized as described in previous reports [12, 23], and purified to avoid unnecessary peaks that are due to side reaction with impurities of the synthesized AQC. The reagent is also commercially available from Waters (Waters corp., Milford, MA). For derivatization, the AQC powder was dissolved in dry acetonitrile to provide a 3 mg/ml solution (about 10 mM).

Materials

Small glass tubes (6×32 mm, Crimp Top Vials, P/N: 03-CVG, Chromacol, UK) for samples and glass vials (27.75× 70 mm, P/N: 224832, Wheaton, NJ) as hydrolysis vessels were pyrolyzed before use at 550 °C for 3 h to remove organic substances. Mininert valves (No. SC-24, P/N: 10130, Pierce, IL) were used for vacuum sealing of the glass vials before hydrolysis. The sample vials were heated by a heat block bath (Thermo Alumi bath ALB-121, Scinics Corporation, Tokyo, Japan) at hydrolysis.

Sample preparations

One-dimensional SDS-PAGE and electroblotting

One-dimensional SDS-PAGE was performed on commercial pre-cast gels (8×8×0.1 cm, 12 wells, 5–20 % gradient; Bio Craft Co., Ltd., Tokyo, Japan). The BSA or TG solution was mixed with an equal volume of sample buffer (125 mM Tris–HCl, pH 6.8; 4 % SDS; 20 % glycerol; 0.2 M DTT; and 0.0125 % bromophenol blue). Aliquots of the mixed solutions were loaded onto individual lanes of polyacrylamide gels and separated by electrophoresis at 10 mA for 3 h at room temperature.

Electroblotting onto a PVDF membrane (ProBlott, Applied Biosystems, Life Technologies Co., Carlsbad, CA) was carried out using a tank blotting procedure (KS-8451, System Instruments Co. Ltd., Tokyo, Japan). Before electroblotting, the PVDF membrane was wetted in methanol and was equilibrated in CAPS transfer buffer (10 mM CAPS and 10 % methanol at pH 11.0) [25]. Blotting in CAPS transfer buffer is useful in reducing the level of Tris and glycine contamination from the polyacrylamide gel. The membrane was handled with gloves and forceps to avoid contamination from skin proteins. After electrophoresis, the gel and the membrane were sandwiched between gel blot papers (GB-003; Whatman, GE Healthcare) and were placed in the blotting cassette in an ice box. Electroblotting was carried out for 15 min at 0.5 A (constant current) in the CAPS transfer buffer. Then, the membrane was rinsed in Milli-Q water, stained with 0.2 % CBB for 1 min, and destained in the mixture of 50 % methanol and 7.5 % acetic acid at room temperature. The membrane was finally rinsed in Milli-Q water, air-dried in a glove box, and stored in doubled-over plastic bags in a refrigerator. In the glove box, the electroblotted bands of BSA or TG on PVDF membranes were excised over the inner plastic bag and rinsed with 50 % acetonitrile in water before treatment with 20 mM HCl. Each piece of the membrane was placed in the hydrolysis tube containing 50 pmol of norvaline as an internal standard.

Solution samples

In the glove box, aliquot of BSA solution was placed in the hydrolysis tube containing 50 pmol of norvaline as an internal standard.

Gas-phase hydrolysis

The hydrolysis tubes containing the sample on the PVDF membrane or in solution were set to a container with a cover and brought into an oxygen-free chamber for hydrolysis that we constructed. The chamber is under positive pressure of nitrogen to prevent oxidation of samples and to prevent contamination from the environment. After the sample container was brought in it, hydrolysis procedures were started when oxygen level in the chamber reached less than 0.1 % detected by an oxygen monitor (JKO-O2LD II, JIKCO Ltd., Tokyo, Japan). The chamber is an appropriate glove box that includes stuff needed for hydrolysis: a vacuum line, a

centrifugal concentrator, the heat block bath, and reagents for hydrolysis. The samples in the hydrolysis tubes were dried by the centrifugal concentrator with the vacuum line. The dried tubes were placed in the glass vial containing 200 μl of constant-boiling HCl and a piece of phenol crystal. Then the vial was sealed under vacuum using the Mininert valve and heated at 110 °C for 20 h by the heat block bath [16, 23]. After hydrolysis, the sample tubes were dried under vacuum.

Derivatization of amino acids

A standard solution containing a mixture of 50 pmol of standard amino acids and norvaline, and the hydrolysate of the BSA solution were derivatized by AQC as previously described [16, 23]. The hydrolysate of BSA or TG from the blotted band was derivatized by adding the AQC solution directly into the hydrolysis tubes containing the PVDF membrane, as follows: The membrane was wetted with 5 μl of acetonitrile, and then, 10 μl of 20 mM HCl was added and vigorously stirred to extract the hydrolysate. Borate buffer (25 μl and 0.2 M at pH 8.8) was added, mixed, and finally 10 μl of the AQC solution was added. The reaction mixtures were stirred immediately. After the mixtures were left to stand for 1 min at room temperature, they were heated at 55 °C for 10 min. The derivatized solution was transferred to a new tube before chromatographic analysis to avoid adsorption of amino acids onto the membrane and piercing of the membrane by a needle of the autosampler. A tenth of the derivatized solution was analyzed by high-performance liquid chromatography (HPLC) as described in the next section.

Analytical procedures

Chromatography

AQC-amino acids of the hydrolysates and the standard solution of amino acids were separated by ion-pair chromatography using a reversed-phase column [16, 26]. An Agilent HPLC system for ultra-high-pressure use (1200 SL series, pressure resistance=600 bar) equipped with binary pumps, a column oven, an autosampler, and a fluorescence detector (excitation at 250 nm and emission at 395 nm) was used. In this system, fluorescence signal can be amplified by increasing the voltage applied to the photomultiplier of the fluorescence detector. We used middle-range voltage, except for obtaining the chromatogram of the 5-fmol amino acid standard solution, in which signals were amplified by approximately a factor of 10 against other measurements. The column used was an InertSustain C18HP column suitable for ultra-high pressure (pressure resistance=500 bar), 3 μm, 3.0×250 mm (GL Sciences Inc, Tokyo, Japan). Elution buffer A was 95 % of 30 mM phosphate buffer (pH 7.3) containing 5 mM TBA-Br as the ion-pair reagent and 5 % acetonitrile, whereas elution buffer B was 50 % of 30 mM phosphate buffer (pH 7.3) with 50 % acetonitrile. The different two elution programs were used based on column condition: linear increases from 2 % B at time 0 to 7.3 % B at 2.7 min, and then to 72.3 % B at 26 min or to 72.3 % B at 35.4 min, followed by a wash with 99 % B for 1.8 min and re-equilibration with 2 % B for 12.4 min. The column was kept at 42 °C, the flow rate was 0.4 ml/min, and the injected volume of the solution of AQC-derivatized amino acids was 5 μl.

Quantification

Under the conditions of conventional acidic hydrolysis, Asn and Gln are completely hydrolyzed to Asp and Glu, respectively, and Trp, Cys, and cystine are partially destroyed [27]. We quantified Asp as the sum of Asp and Asn and Glu as the sum of Glu and Gln. For quantitative analysis, 50 pmol of the standard solution containing 17 amino acids (other than Trp, Asn, and Gln) was derivatized by the same procedure used with the hydrolyzed samples. A tenth of the total hydrolysate of the standard solution was injected onto the column. We evaluated the amounts of 17 amino acids in the samples by calculating the ratio of the peak height of an amino acid in the sample to that of the same amino acid in the standard. Total weight of amino acids was calculated by sum of multiplying the obtained amounts of amino acids by each residual mass. In all experiments for protein quantification, each sample was hydrolyzed and analyzed three times, and the standard deviation of the means was calculated as $(\Sigma(\text{experimental value}-\text{average value})^2/2)^{1/2}$.

Method validation

We derivatized 150 pmol of the amino acid standard, and the derivatized solution was diluted to make a dilution series of the standard. By plotting the quantified amount of AQC-Arg against the injected amount of AQC-Arg, we ascertained the linear range and the LOD (limit of detection) of the fluorescence detector. We defined the minimum amount that maintained the linear response as the LOQ (limit of quantification).

We validated the quantitative accuracy of AAA by protein identification using the amino acid compositions derived from the analyses and a search program of a protein database. For the Swiss-Prot database search, the ExPASy AACompIdent tool was used (http://web.expasy.org/aacompident/) with constellation 2 (Asp+Asn=Asx, Gln+Glu=Glx, and Cys and Trp are not considered) chosen without any limit of species, isoelectric point, or molecular weight of the proteins. Proteins, at amounts ranging from a

few nanograms to several tens of nanograms, were quantified and validated. We defined the minimum quantity of protein that was identified correctly by the database search as the LOH (limit of handling).

Results and discussion

Chromatographic analysis of amino acids

Pre-column derivatization with fluorescent molecules enhances the hydrophobicity of amino acids and enables separation of amino acids by reversed-phase liquid chromatography (RPLC), resulting in faster analysis and higher sensitivity than that of conventional ion-exchange chromatography. In the case of RPLC, hydrophilic molecules elute earlier, and hydrophobic molecules are eluted later, with progressive elution at increasing ratios of organic solvents. In general, the fluorescence intensity of eluted compounds is stronger in hydrophobic circumstances. Therefore, in the case of fluorescence detection of eluted samples of RPLC, the fluorescence intensity of samples that are eluted later is stronger. The solvent effect leads to a different response factor for each amino acid, and the peak-areas of amino acids that are eluted earlier are almost one fifth smaller than the later one [12]. It is more difficult to quantify the amino acids with small response factors rather than those with large response factors especially in extremely small amount of samples. To circumvent this issue, we used an ion-pair reagent to enhance the hydrophobicity of the AQC-derivatives of hydrophilic amino acids and to reduce the solvent effect [26]. By application of the latest ultra-high-pressure LC, we were able to use a long column with small internal diameter and to improve theoretical plate-number and signal-to-noise ratio of chromatograms resulting in high sensitivity with excellent resolution. Figure 1 represents the typical chromatogram of 5 fmol of the AQC-amino acid standard (after subtraction of the chromatogram of the blank/water).

Quantification of small amounts of amino acids

The sensitivity and linear response range of the detector need to be adequate enough to quantify small amounts of proteins. These requirements depend on the two kinds of limitations dependent on the performance of the fluorescence detector, LOD and LOQ. Usual photomultipliers, including those in fluorescence detectors, have a linear response range of two to four orders of sample quantities against the intensity of incident light. Because the response is not linear at both ends of the intensity plot, at the lowest and highest intensities of incident light, the amounts of amino acids cannot be quantified accurately even if the

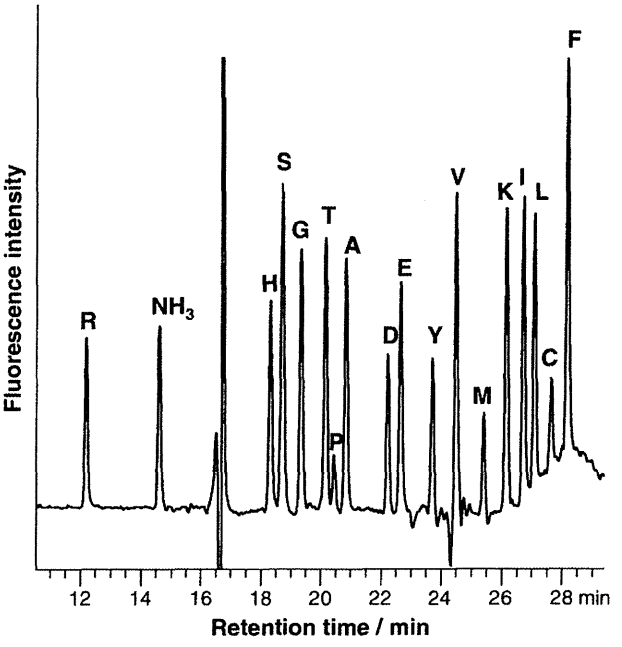

Fig. 1 Typical chromatogram of AQC-amino acid standards of 5 fmol that subtracted a blank chromatogram of injection of water (gradient condition, 2–7.3–72.3 % B/0–2.7–26 min)

signals are detectable. We defined the sample limit at which the linear response is maintained as the LOQ and the lower limit at which the signal from the amino acids is still detectable as the LOD. We evaluated LOQ and LOD by measuring the detector response to a dilution series of AQC-Arg standards. The amounts of the AQC-Arg quantified are plotted against the injected amounts of AQC-Arg in Fig. 2. For our chromatographic condition and detection system, almost four-order linearity from 0.6 fmol to 5 pmol was observed, which means that the LOQ was 0.6 fmol. In contrast, the LOD was 50 amol, as shown in Fig. 2.

Recent developments in MS have enabled highly sensitive detection of free amino acids, and MS has also been used for AAA. There are basically two main methods to detect amino acids by MS. One of them is a non-labeling method, in which the amino acids are detected without derivatization. Miyano et al. [28] reported that the LOD of the non-labeling-based MS detection was 10–90 fmol. Another MS method is the pre-label method in which the amino acids are derivatized with reagents that are selectively cleaved during ionization and generate the same fragment for selective reaction monitoring (SRM). The pre-label method achieved an LOD of femtomoles to several tens of attomoles [14, 15]. Since the advantages of SRM-MS are high selectivity and short analysis time, SRM-MS is suitable for metabolomics. To use these MS methods for quantification of amino acids, however, expensive equipment and stable isotope-labeled amino acids are needed, resulting in

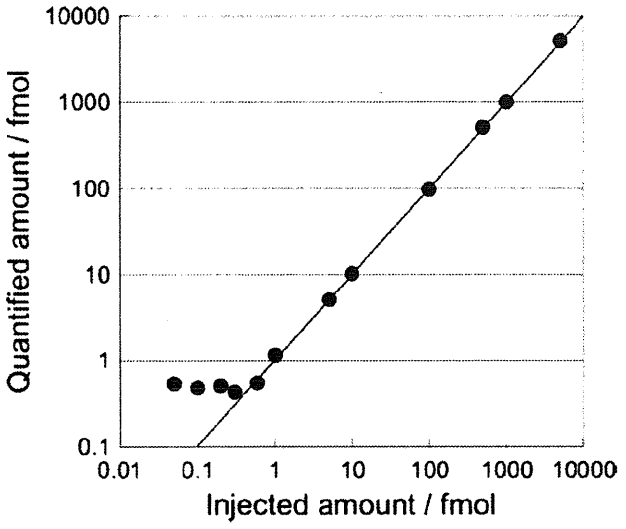

Fig. 2 Quantified amount of AQC-Arg was plotted against injected amount. Linearity of detector response confined the limit of quantification to 0.6 fmol, whereas limit of detection was 0.05 fmol

a high cost. Moreover, detection range for each amino acid is relatively narrow: two to four orders in concentration of amino acids [14].

The quantification of amino acids in proteins is more complicated than that of free amino acids because of the requirement for hydrolysis. The LOQ of amino acids in proteins depends on the quantitative recovery of amino acids via protein hydrolysis.

Actual limit for quantification of small amounts of proteins

For the quantification of small amounts of proteins, not only the LOQ but also the LOH dominates the quantitative results because one more process, hydrolysis, is needed before quantification of the released amino acids. Hydrolysis contains complicated operational steps that create a risk of contamination from the environment to the samples. Appropriate equipment, such as the oxygen-free chamber for hydrolysis, gloves, and forceps, as well as a proper technique for handling small amounts of samples, can prevent the contamination. Generally, a blank sample tube is simultaneously hydrolyzed with protein samples for background correction. Then the contributions from the contamination that are the background peaks of the blank sample are subtracted from the chromatogram of protein sample. However, the contamination to protein samples is not necessarily the same as that to the hydrolysis blank. Furthermore, there is so far no guideline how extent of contamination makes the quantification of proteins end in failure. As a new guideline, we defined the limit of handling accuracy, LOH, and adopted the protein identification by the obtained amino acid compositions and the Swiss-Prot database for evaluation of the LOH.

Table 1 Amino acid contents of BSA

	Theoretical residue number	BSA solution (54 ng)[a] amount (pmol)	BSA solution (16 ng)[a] amount (pmol)	BSA solution (2.6 ng)[a] amount (pmol)	blotted BSA (33 ng)[a] amount (pmol)
Arg (R)	23	19.2±0.47 (24.5)[b]	5.21±0.13 (23.1)[b]	0.855±0.05 (21.0)[b]	11.0±0.28 (23.6)[b]
His (H)	16	13.4±1.00 (17.1)[b]	3.79±0.12 (16.8)[b]	0.618±0.03 (15.2)[b]	6.96±0.10 (14.9)[b]
Ser (S)	28	22.7±0.45 (29.0)[b]	7.97±0.51 (35.3)[b]	2.56±0.01 (63.0)[b]	17.3±0.09 (37.1)[b]
Gly (G)	16	14.9±0.23 (19.0)[b]	6.00±1.20 (26.6)[b]	1.94±0.03 (47.7)[b]	13.3±0.15 (28.5)[b]
Thr (T)	33	27.9±0.68 (35.6)[b]	7.92±0.17 (35.1)[b]	1.35±0.06 (33.2)[b]	16.2±0.02 (34.7)[b]
Pro (P)	28	22.3±0.60 (28.5)[b]	6.5±0.24 (28.6)[b]	1.02±0.04 (25.1)[b]	14.1±0.01 (30.2)[b]
Ala (A)	47	38.6±0.87 (49.3)[b]	11.5±0.12 (50.9)[b]	1.96±0.08 (48.2)[b]	24.2±0.06 (51.9)[b]
Asp (D)	55	44.4±1.40 (56.7)[b]	12.6±0.26 (55.8)[b]	2.27±0.11 (55.9)[b]	26.0±0.02 (55.7)[b]
Glu (E)	79	71.0±1.90 (90.7)[b]	20.4±0.91 (90.3)[b]	3.61±0.17 (88.8)[b]	42.1±0.05 (90.2)[b]
Tyr (Y)	20	14.4±0.28 (18.4)[b]	4.06±0.25 (18.0)[b]	0.729±0.03 (17.9)[b]	9.72±0.12 (20.8)[b]
Val (V)	36	28.3±0.80 (36.2)[b]	8.05±0.23 (35.7)[b]	1.33±0.07 (32.7)[b]	17.2±0.07 (36.9)[b]
Met (M)	4	3.33±0.13 (4.3)[b]	1.27±0.19 (5.6)[b]	0.205±0.00 (5.0)[b]	1.09±0.20 (2.3)[b]
Lys (K)	59	48.6±1.20 (62.1)[b]	13.4±0.22 (59.3)[b]	2.16±0.13 (53.1)[b]	27.3±0.11 (58.5)[b]
Ile (I)	14	10.9±0.31 (13.9)[b]	3.54±0.18 (15.7)[b]	0.760±0.19 (18.7)[b]	6.96±0.10 (14.9)[b]
Leu (L)	61	49.3±1.40 (63.0)[b]	14.0±0.32 (62.0)[b]	2.24±0.11 (55.1)[b]	30.2±0.03 (64.7)[b]
Phe (F)	27	21.7±0.56 (27.7)[b]	6.18±0.14 (27.4)[b]	1.03±0.05 (25.3)[b]	13.3±0.10 (28.5)[b]
Total amount (ng)[c]		52	15	2.7	31

[a] These protein amounts were calculated from average of calculated protein amounts using obtained amounts of A, F, and L

[b] The values in parentheses were calculated residue numbers from the obtained amounts of amino acids

[c] The total amount was calculated by sum of multiplying the obtained amounts of amino acids by each residual mass

We prepared three concentrations of BSA in solution, containing 2.6, 16, and 54 ng of BSA, hydrolyzed the samples, and quantified the constituted amino acids. The amount of amino acids in picomoles and calculated total amount of amino acids in nanograms by the sum of multiplying the obtained amounts of amino acids by each residual mass are listed in Table 1. The calculated residue numbers from the amount of amino acids and molecular weight of BSA were also listed in Table 1. The residue number of the sample with 54 ng of BSA matched the theoretical values, whereas a slight increase was observed in Ser and Gly values for the sample with 16 ng of BSA. We assessed whether analyzed proteins were correctly identified by the Swiss-Prot protein database search without the restriction of species using these obtained composition and the ExPASY AACompIdent program. The results of the database search for 54 and 16 ng of BSA (shown in Table 2) indicated that both the samples were identified as BSA. However, the residue number of 2.6 ng of BSA (listed in Table 1) deviated from the theoretical values, especially for Ser and Gly, and BSA was not hit until a rank of 10. From the results, the LOH was 16 ng, or 240 fmol, of BSA in solution.

The LOQ of amino acids, 0.6 fmol, was one order lower than the obtained LOH. However, the increase of Ser and Gly prevented identification of the much smaller amount of protein such as 2.6 ng for BSA solution. If the database search was performed using the calculated compositions of Ser and Gly derived from the theoretical residue numbers and the observed compositions of other amino acids, 2.6 ng of BSA was successfully identified with a rank of 1. Since the increase of Ser and Gly may be caused from a slight contamination from the environment, the contamination should be excluded or further minimized to accomplish the quantification of 1 ng of protein, such as that achieved effectively by automation of sample preparation and/or sample hydrolysis [23].

Quantification of proteins electroblotted to PVDF membranes

The blotted protein bands are detected by staining with CBB, with a detection limit around 50 ng that sets the least value of LOH. We cut off the protein bands containing 33 ng of BSA or 44 ng of TG, and the proteins were hydrolyzed on the membrane. The obtained amounts and calculated residue numbers of amino acids of the blotted BSA are listed in Table 1. In Fig. 3, the chromatogram of the hydrolysate of the blotted TG is shown. The injected amount of TG was one-tenth of the hydrolysate, i.e., 4.4 ng (14.5 fmol). We

Table 2 The closest Swiss-Prot entries from the ExPASy AACompIdent program without the restriction of species, isoelectric point (p*I*), and molecular weight (Mw)

Rank	Score	Protein	p*I*	Mw	Description
BSA solution (54 ng)					
1	2	ALBU_BOVIN	5.6	66,433	Serum albumin
2	6	ALBU_SHEEP	5.58	66,328	Serum albumin
3	11	ALBU_RAT	5.8	65,916	Serum albumin
4	11	ALBU_PIG	5.84	66,798	Serum albumin
5	11	ALBU_MOUSE	5.53	65,892	Serum albumin
BSA solution (16 ng)					
1	6	ALBU_BOVIN	5.6	66,433	Serum albumin
2	11	ALBU_SHEEP	5.58	66,328	Serum albumin
3	12	ALBU_RAT	5.8	65,916	Serum albumin
4	13	ALBU_MOUSE	5.53	65,892	Serum albumin
5	14	ALBU_HORSE	5.72	65,752	Serum albumin
Blotted BSA (33 ng)					
1	7	ALBU_BOVIN	5.6	66,433	Serum albumin
2	12	ALBU_SHEEP	5.58	66,328	Serum albumin
3	13	ALBU_MOUSE	5.53	65,892	Serum albumin
4	14	ALBU_RAT	5.8	65,916	Serum albumin
5	14	ALBU_HORSE	5.72	65,752	Serum albumin
Blotted TG (44 ng)					
1	5	THYG_BOVIN	5.5	301,219	Thyroglobulin
2	11	THYG_HUMAN	5.42	302,728	Thyroglobulin
3	15	MNMC_IDILO	5.54	67,069	tRNA
4	16	THYG_MOUSE	5.32	302,414	Thyroglobulin
5	17	THYG_RAT	5.04	30,252	Thyroglobulin

The program constellation 2 (Asp+Asn=Asx, Gln+Glu=Glx, and Cys and Trp are not considered) was used

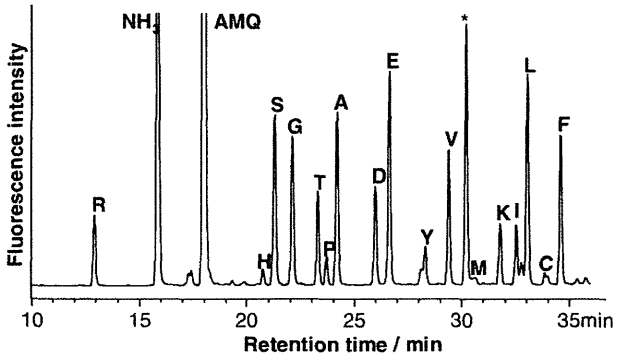

Fig. 3 Chromatogram of hydrolysate of blotted TG. A blotted band that contains 44 ng (145 fmol) of TG was hydrolyzed and a tenth of them were injected. AMQ abbreviates 6-aminoquinoline that is formed by hydrolysis of AQC. The *asterisk*-marked peak is an internal standard, norvaline (gradient condition, 2–7.3–72.3 % B/0–2.7–35.4 min)

verified the quantitative accuracy by performing the database search using the obtained amino acid composition. The composition matched the theoretical value, and the database search identified the protein bands as BSA or TG with a rank of 1 as shown in Table 2. The results mean the least value of LOH that is determined by the CBB detection limit was achieved in this study. The obtained LOH value for the electroblotted samples was the same extent as solution samples.

In a previous report, Murayama et al. [17] analyzed a part of the hydrolysate of a protein electroblotted onto PVDF, which was 2.4 fmol of multidrug-resistant protein 1 (MDR1, 160 kDa), and successfully identified it. However, they hydrolyzed an amount of MDR1 1,000 times larger than the injected amount to eliminate the influence of contamination. In other words, the LOH was 2.4 pmol in their case, although 2.4 fmol of MDR1 was identified. In another report, Cohen et al. collected purified proteins by capillary electrophoresis onto PVDF membranes and hydrolyzed 100–700 ng of the collected proteins on the PVDF membranes. They reported that amino acid compositions of 100–700 ng of proteins were obtained with average errors 9.9–21.3 % [24]. They also pointed the average errors rose rapidly (30–60 %) for 60 ng hydrolyzed samples. In our method, accurate AAA was accomplished for an order of small amount of proteins by accumulating small improvements in handling. For hydrolysate of 33 ng of BSA or 44 ng of TG on PVDF membrane, the average errors in the amino acid composition observed was 12 %. Since percent recovery of blotted BSA from amount on SDS-PAGE gel were reported as 35 % [29], 94 ng of BSA is needed as starting amount for SDS-PAGE.

Conclusions

We improved the sensitivity of AAA to the following specifications; an LOD of 50 amol, an LOQ of 0.6 fmol, and four orders of linearity. Critical manipulation before hydrolysis was done in the oxygen-free chamber under positive pressure of nitrogen to prevent oxidation of samples and to keep out dust.

In order to evaluate the LOH of proteins the protein identification was performed with the Swiss-Prot database search using the obtained compositions of amino acids and the ExPASy AACompIdent tool. As a result, hydrolysates from solution containing 16 ng (240 fmol) of BSA, a PVDF membrane with 33 ng (500 fmol) of electroblotted BSA, and a PVDF membrane with 44 ng (145 fmol) of electroblotted TG were successfully identified. The LOH was less than one-tenth of that reported previously [17]. This method was practical for the quantification of proteins, at less than 100 ng either in solution or on PVDF membranes. In the case of 2.6 ng of BSA, the increase in Ser and Gly prevented identification of the protein. Thus a limitation of manual hydrolysis, namely the LOH, was likely a result of contamination with Ser and Gly from the environment. For further highly sensitive analysis, automation of sample preparation and/or sample hydrolysis will be effective in suppressing contamination and facilitating the quantification of 1 ng of proteins.

Acknowledgments This work was supported in part by a Grant-in-Aid from the Ministry of Health, Labor and Welfare of Japan and the Chemical Genomics Research Project, RIKEN Advanced Science Institute (ASI), and by an Incentive Research Grant from RIKEN ASI.

References

1. Matsumoto K, Nakayama H, Yoshimura M, Masuda A, Dohmae N, Matsumoto S, Tsujimoto M (2012) RNA Biol 9:610–623
2. Unoki M, Masuda A, Dohmae N, Arita K, Yoshimatsu M, Iwai Y, Fukui Y, Ueda K, Hamamoto R, Shirakawa M, Sasaki H, Nakamura Y (2013) J Biol Chem 288:6053–6062
3. Tsukazaki T, Mori H, Fukai S, Ishitani R, Mori T, Dohmae N, Perederina A, Sugita Y, Vassylyev DG, Ito K, Nureki O (2008) Nature 455:988–991
4. Kaspar H, Dettmer K, Gronwald W, Oefner PJ (2009) Anal Bioanal Chem 393:445–452
5. Steven L, Cohen M (2005) In: Molnár-Perl I (ed) Quantitation of amino acids and amines by chromatography (Journal of chromatography library, Vol.70). Elsevier, Amsterdam
6. Wilkins MR, Yan JX, Gooley AA (1999) Methods Mol Biol 112:445–460
7. Moore S, Stein WH (1951) J Biol Chem 192:663–681
8. Moore S, Stein WH (1954) J Biol Chem 211:893–906
9. Watanabe Y, Imai K (1981) Anal Biochem 116:471–472
10. Einarsson S, Josefsson B, Lagerkvist S (1983) J Chromatogr A 282:609–618
11. Lindroth P, Mopper K (1979) Anal Chem 51:1667–1674
12. Cohen SA, Michaud DP (1993) Anal Biochem 211:279–287
13. Kaspar H, Dettmer K, Chan Q, Daniels S, Nimkar S, Daviglus ML, Stamler J, Elliott P, Oefner PJ (2009) J Chromatogr B Analyt Technol Biomed Life Sci 877:1838–1846

14. Shimbo K, Yahashi A, Hirayama K, Nakazawa M, Miyano H (2009) Anal Chem 81:5172–5179
15. Armenta JM, Cortes DF, Pisciotta JM, Shuman JL, Blakeslee K, Rasoloson D, Ogunbiyi O, Sullivan DJ Jr, Shulaev V (2010) Anal Chem 82:548–558
16. Masuda A, Dohmae N (2011) Biosci Trends 5:231–238
17. Shindo N, Fujimura T, Nojima-Kazuno S, Mineki R, Furusawa S, Sasaki K, Murayama K (1998) Anal Biochem 264:251–258
18. Cohen S A, De Antonis K, Michaud D P (1993) In: Angeletti R H (ed) Techniques in protein chemistry IV. Academic, San Diego
19. Bidlingmeyer BA, Tarvin TL, Cohen SA (1987) In: Walsh K A (ed) Methods in protein sequence analysis. Humana Press, Clifton, pp. 229–245
20. Hunziker P, Andersen TT, Bao Y, Cohen SA, Denslow ND, Hulmes JD, Mahrenholz AM, Mann K, Schegg KM, West KA, Crabb JW (1999) J Biomol Tech 10:129–136
21. Tous GI, Fausnaugh JL, Akinyosoye O, Lackland H, Winter-Cash P, Vitorica FJ, Stein S (1989) Anal Biochem 179:50–55
22. Kawahara-Kobayashi A, Masuda A, Araiso Y, Sakai Y, Kohda A, Uchiyama M, Asami S, Matsuda T, Ishitani R, Dohmae N, Yokoyama S, Kigawa T, Nureki O, Kiga D (2012) Nucleic Acids Res 40:10576–10584
23. Masuda A, Dohmae N (2010) Anal Chem 82:8939–8945
24. Cohen SA, Warren WJ (1994) In: Crabb JW (ed) Techniques in protein chemistry V. Academic, San Diego
25. Matsudaira P (1987) J Biol Chem 262:10035–10038
26. Shindo N, Nojima S, Fujimura T, Taka H, Mineki R, Murayama K (1997) Anal Biochem 249:79–82
27. Fountoulakis M, Lahm HW (1998) J Chromatogr A 826:109–134
28. Yoshida H, Mizukoshi T, Hirayama K, Miyano H (2007) J Agric Food Chem 55:551–560
29. Wong S, Padua A, Henzel WJ (1992) In: Angeletti RH (ed) Techniques in protein chemistry III. Academic, San Diego

Contents lists available at ScienceDirect

Biochemical and Biophysical Research Communications

journal homepage: www.elsevier.com/locate/ybbrc

Specific inhibition of hepatitis C virus entry into host hepatocytes by fungi-derived sulochrin and its derivatives

Syo Nakajima [a,b], Koichi Watashi [a,b,c], Shinji Kamisuki [b], Senko Tsukuda [a,b], Kenji Takemoto [b], Mami Matsuda [a], Ryosuke Suzuki [a], Hideki Aizaki [a], Fumio Sugawara [b], Takaji Wakita [a]

[a] Department of Virology II, National Institute of Infectious Diseases, Tokyo 162-8640, Japan
[b] Tokyo University of Science Graduate School of Science and Technology, Noda 278-8510, Japan
[c] Micro-Signaling Regulation Technology Unit, RIKEN Center for Life Science Technologies, Wako 351-0198, Japan

ARTICLE INFO

Article history:
Received 5 September 2013
Available online 5 October 2013

Keywords:
HCV
Entry
Sulochrin
Natural product
Screening
Compound

ABSTRACT

Hepatitis C virus (HCV) is a major causative agent of hepatocellular carcinoma. Although various classes of anti-HCV agents have been under clinical development, most of these agents target RNA replication in the HCV life cycle. To achieve a more effective multidrug treatment, the development of new, less expensive anti-HCV agents that target a different step in the HCV life cycle is needed. We prepared an in-house natural product library consisting of compounds derived from fungal strains isolated from seaweeds, mosses, and other plants. A cell-based functional screening of the library identified sulochrin as a compound that decreased HCV infectivity in a multi-round HCV infection assay. Sulochrin inhibited HCV infection in a dose-dependent manner without any apparent cytotoxicity up to 50 μM. HCV pseudoparticle and trans-complemented particle assays suggested that this compound inhibited the entry step in the HCV life cycle. Sulochrin showed anti-HCV activities to multiple HCV genotypes 1a, 1b, and 2a. Co-treatment of sulochrin with interferon or a protease inhibitor telaprevir synergistically augmented their anti-HCV effects. Derivative analysis revealed anti-HCV compounds with higher potencies (IC_{50} < 5 μM). This is the first report showing an antiviral activity of methoxybenzoate derivatives. Thus, sulochrin derivatives are anti-HCV lead compounds with a new mode of action.

1. Introduction

Hepatitis C virus (HCV) infection is a major causative agent of chronic liver diseases such as liver cirrhosis and hepatocellular carcinoma [1]. The standard anti-HCV therapy has been a co-treatment with pegylated-interferon (IFN)α and ribavirin, but this therapy is limited by less efficacy to certain HCV genotypes, poor tolerability, serious side effects, and high cost [2,3]. In addition to the newly approved protease inhibitors, telaprevir and boceprevir, a variety of anti-HCV candidates are under clinical development. Although these drugs improve the virological response rate, the emergence of drug-resistant virus is expected to be a significant problem. Moreover, these compounds are expensive due to their complex structure and the many steps required for their total synthesis. To overcome the drug-resistant virus and achieve a long-term antiviral effect, multidrug treatment is essential. Thus, the development of drugs targeting a different step in the HCV life cycle and presumably requiring low cost is urgently needed.

HCV propagates in hepatocytes through its viral life cycle including: attachment and entry (defined as the early step in this study); translation, polyprotein processing, and RNA replication (the middle step); and assembly, trafficking, budding, and release (the late step) (Supplementary Fig. S1). The middle step has been extensively analysed, especially after the establishment of the HCV replicon system [4]. The early step can be analysed with HCV pseudoparticle (HCVpp) [5,6], which is a murine leukemia virus- or human immunodeficiency virus-based pseudovirus carrying HCV E1 and E2 as envelope proteins. The HCV-producing cell culture system (HCVcc) is used for analyzing the whole life cycle [7–9]. In addition, the HCV trans-complemented particle (HCVtcp) system carrying an HCV subgenomic replicon RNA packaged in HCV E1 and E2-containing particles can evaluate the life cycle from the early to the middle step [10]. The majority of anti-HCV agents currently under clinical development, such as inhibitors of protease, polymerase, NS5A, and cellular cyclophilin, inhibit polyprotein processing and/or RNA replication. A desirable approach

Abbreviations: HCV, hepatitis C virus; IFN, interferon; HCVpp, HCV pseudoparticle; HCVcc, HCV derived from cell culture; HCVtcp, HCV trans-complemented particle; MOI, multiplicity of infection; HBs, HBV envelope protein; CsA, cyclosporin A; VSV, vesicular stomatitis virus.

* Corresponding author. Adress: Department of Virology II, National Institute of Infectious Diseases, 1-23-1 Toyama, Shinjuku-ku, Tokyo 162-8640, Japan. Fax: +81 3 5285 1161.
E-mail address: kwatashi@nih.go.jp (K. Watashi).

0006-291X/$ - see front matter © 2013 Elsevier Inc. All rights reserved.
http://dx.doi.org/10.1016/j.bbrc.2013.09.100

to achieving efficient multidrug therapy is to identify new antiviral drugs targeting different steps in the viral life cycle. A combination of drugs with different targets can greatly decrease the emergence of drug-resistant virus.

Natural products generally contain more characteristics of high chemical diversity than combinatorial chemical collections, and therefore have a wider range of physiological activities [11,12]. They offer major opportunities for finding novel lead structures that are active in a biological assay. Moreover, biologically active natural products are generally small molecules with drug-like properties, and thus development costs of producing orally active agents tend to be lower than that derived from combinatorial chemistry [13]. In addition, there is a wide variety of natural compounds reported to possess antiviral activity [14,15]. In the present study, we have taken advantage of the potential of natural products by screening a natural product library derived from fungal extracts with a cell-based assay that supports the whole life cycle of HCV.

2. Materials and methods

2.1. Cell culture

Huh-7.5.1 [8] and HepaRG cells [16] were cultured as described previously.

2.2. Natural product library and reagents

Natural products were extracted essentially as previously described [17]. Culture broths of fungal strains isolated from seaweeds, mosses, and other plants were extracted with CH_2Cl_2. The crude extracts were separated by silica gel column chromatography to purify compounds. The chemical structure of each compound was determined by NMR and mass spectrometry analyses. Thus, we prepared an in-house natural product library consisting of approximately 300 isolated compounds.

Cyclosporin A was purchased from Sigma. Bafilomycin A1 and chlorpromazine were purchased from Wako. Heparin was obtained from Mochida Pharmaceutical. IFNα was purchased from Schering-Plough.

2.3. Compound screening

Huh-7.5.1 cells were treated with HCV J6/JFH1 at a multiplicity of infection (MOI) of 0.15 for 4 h. The cells were washed and then cultured with growth medium treated with 10 μM of each compound for 72 h. The infectivity of HCV in the medium was quantified. Cell viability at 72 h post-treatment was simultaneously measured. Compounds that decreased the cell viability to less than 50% of that without treatment were eliminated for further evaluations. Normalised infectivity was calculated as HCV infectivity divided by cell viability. Compounds reducing the normalised infectivity to less than 40% were selected as initial hits. The initial hits were further evaluated for data reproduction and dose-dependency.

2.4. HCVcc assay

HCVcc was recovered from the medium of Huh-7.5.1 cells transfected with HCV J6/JFH-1 RNA as described [7]. HCVcc was infected into Huh-7.5.1 cells at 0.15 MOI for 4 h. After washing out the inoculated virus, the cells were cultured with normal growth medium in the presence or absence of compounds for 72 h. The infectivity of HCV and the amount of HCV core protein in the medium were quantified by infectious focus formation assay and chemiluminescent enzyme immunoassay (Lumipulse II HCV core assay, ortho clinical diagnostics), respectively [7,18].

2.5. Immunoblot analysis

Immunoblot analysis was performed as described previously [19]. The anti-HCV core antibody (2H9) was used as a primary antibody with 1:1000 dilution [7].

2.6. MTT assay

The viability of cells was quantified by using a Cell Proliferation Kit II XTT (Roche Diagnostics) as described previously [20].

2.7. HCV replicon assay

Huh-7.5.1 cells were transfected with an HCV subgenome replicon RNA (SGR–JFH1/Luc) for 4 h and then incubated with or without compounds for 48 h [21]. The cells were lysed with 1xPLB (Promega), and the luciferase activity was determined with a luciferase assay system (Promega) according to the manufacturer's protocol [22].

2.8. HCVpp assay

HCVpp was recovered from the medium of 293T cells transfected with expression plasmids for HCV JFH-1 E1E2, MLV Gag-Pol, and luciferase, which were kindly provided from Dr. Francois-Loic Cosset at Universite de Lyon [5]. Vesicular stomatitis virus pseudoparticles (VSVpp) was similarly recovered with transfection by replacing HCV E1E2 with VSV G.

Huh-7.5.1 cells were preincubated with compounds for 3 h and were then infected with HCVpp in the presence of compounds for 4 h. After washing out virus and compounds, cells were incubated for an additional 72 h before recovering the cell lysates and quantifying the luciferase activity.

2.9. HCVtcp assay

The HCVtcp assay was essentially performed as described [10]. Briefly, Huh-7 cells were transfected with expression plasmids for the HCV subgenomic replicon carrying the luciferase gene and for HCV core-NS2 based on genotype 1a (RMT) (kindly provided by Dr. Michinori Kohara at Tokyo Metropolitan Institute of Medical Science), 1b (Con1), and 2a (JFH-1) [4,10,23] to recover HCVtcp. HCVtcp can reproduce RNA replication as well as HCV-mediated entry into the cells [10].

2.10. Synergy analysis

To determine whether the effect of the drug combination was synergistic, additive, or antagonistic, MacSynergy (kindly provided by Mark Prichard), a mathematical model based on the Bliss independence theory, was used to analyse the experimental data shown in Fig. 3A. In this model, a theoretical additive effect with any given concentrations can be calculated by $Z = X + Y(1-X)$, where X and Y represent the inhibition produced by each drug alone, and Z represents the effect produced by the combination of two compounds if they were additive. The theoretical additive effects were compared to the actual experimental effects at various concentrations of the two compounds and were plotted as a three-dimensional differential surface that would appear as a horizontal plane at 0 if the combination were additive. Any peak above this plane (positive values) indicates synergy, whereas any depression below the plane (negative values) indicates antagonism. The 95% confidence interval of the experimental dose–response was considered to reveal only effects that were statistically significant.

3. Results

3.1. Screening of natural products possessing anti-HCV activity

We extracted culture broths of fungal strains isolated from seaweeds, mosses, and other plants and purified compounds as described in the Section 2 [17]. The chemical structure of each compound was determined by NMR and mass spectrometry analyses. Thus, we prepared an in-house natural product library consisting of approximately 300 isolated compounds. As shown in the Section 2, compounds reducing the normalised HCV infectivity to less than 40% as compared with DMSO were selected as primary hits. The primary hits were then validated by examining the reproducibility, dose-dependency, and cell viability in the HCVcc system. Sulochrin [methyl 2-(2,6-dihydroxy-4-methylbenzoyl)-5-hydroxy-3-methoxybenzoate] (Fig. 1A) was one of the compounds showing the highest anti-HCV activity, and the following analyses focus mainly on this compound.

3.2. Sulochrin decreased HCV infectivity in HCV cell culture assay

To characterise the anti-HCV activity of the compounds, Huh-7.5.1 cells were infected with HCV J6/JFH1 at an MOI of 0.15 and then cultured for 72 h in the presence or absence of compounds.

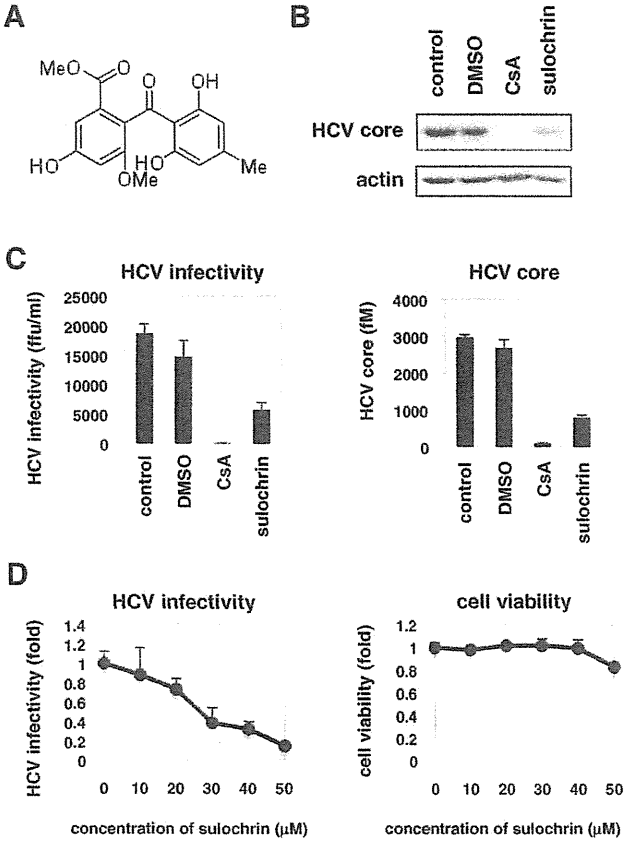

Fig. 1. Sulochrin decreased HCV production in a multi-round HCV infection assay. (A) Chemical structure of sulochrin. (B) Huh-7.5.1 cells were infected with HCV J6/JFH-1 at an MOI of 0.15 for 4 h and then incubated with or without 0.3% DMSO, 2 μM cyclosporin A (CsA), or 30 μM sulochrin for 72 h. The resultant medium was inoculated into naïve Huh-7.5.1 cells to detect intracellular HCV core and actin protein at 48 h postinoculation by immunoblot. (C) HCV infectivity (left) and HCV core protein (right) in the medium as prepared in (B) were quantified as shown in the Section 2. (D) HCV infectivity (left) determined as shown in (C) with varying concentrations (0–50 μM) of sulochrin. Cell viability was examined by MTT assay (right).

In this system, infectious HCV is secreted into the medium and then re-infects into uninfected cells to support the spread of HCV during a 72 h period (Section 2). Cell cultures were treated with sulochrin or cyclosporin A (CsA) as a positive control in this mul-

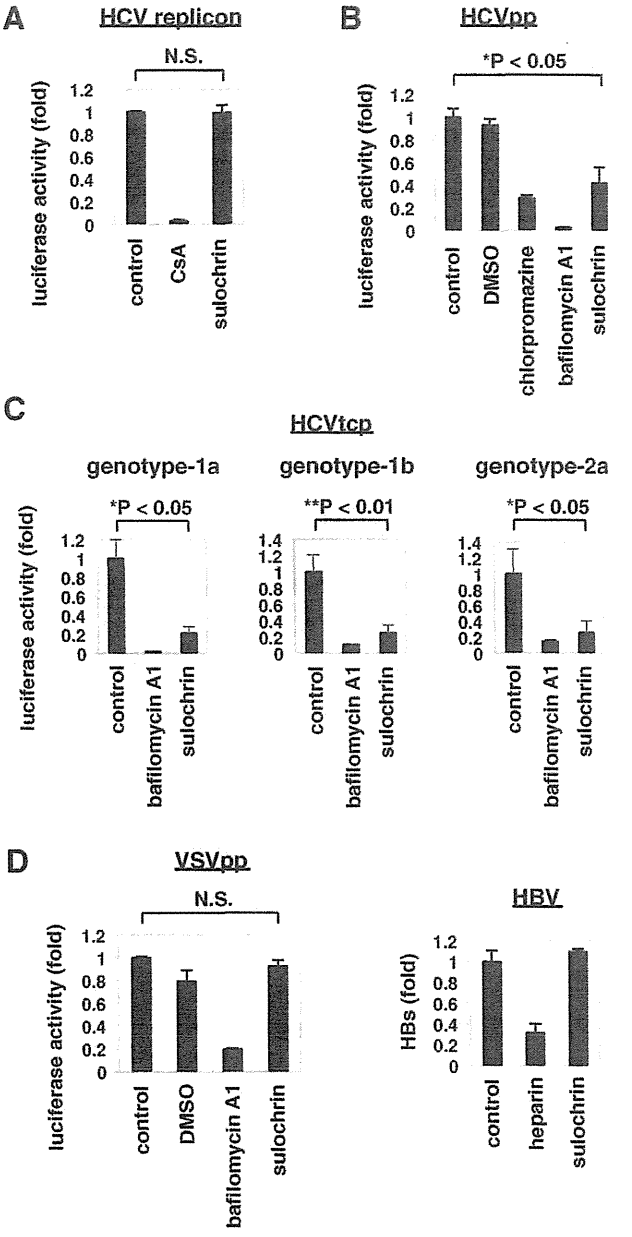

Fig. 2. Sulochrin blocked HCV entry. (A) Replicon assay. Huh-7.5.1 cells were transfected with an HCV subgenomic replicon RNA for 4 h followed by treatment with or without the indicated compounds for 48 h. Luciferase activity driven by the replication of the subgenomic replicon was quantified. (B and C) HCV pseudoparticle (HCVpp) and trans-complemented particle (HCVtcp) assay. Huh-7.5.1 cells were pretreated with the indicated compounds for 3 h and then infected with HCVpp (B) or HCVtcp (C) for 4 h. After washing out virus and compounds, cells were further incubated for 72 h and harvested for measuring luciferase activity driven by the infection of HCVpp or HCVtcp. HCVtcp assay was performed with HCV E1 and E2 derived from genotypes 1a (RMT), 1b (Con1), and 2a (JFH1). (D) Left, the pseudoparticle assay was performed as shown in (B) with VSV G instead of HCV E1 and E2. Right, HBV infection assay. HepaRG cells were pretreated with the indicated compounds for 3 h and then infected with HBV for 16 h. After washing out virus and compounds, cells were incubated for an additional 12 days. HBV infection was evaluated by measuring HBs secretion from the infected cells. Heparin was used as a positive control that inhibits HBV entry.

ti-round infection system. To examine the level of infectious HCV particles produced from the cells, the resultant medium was inoculated into naive Huh-7.5.1 cells to detect HCV core protein in the cells. As shown in Fig. 1B, intracellular production of HCV core but not that of actin was reduced in the cells inoculated with sulochrin- and CsA-treated medium (Fig. 1B). Quantitative analysis showed that sulochrin decreased HCV infectivity and HCV core protein in the medium to 1/3–1/4 of the untreated levels (Fig. 1C). Reduction of HCV infectivity by sulochrin was dose-dependent without serious cytotoxicity up to 50 μM (Fig. 1D).

3.3. Sulochrin blocked HCV entry

We investigated the step in the HCV life cycle that was inhibited by sulochrin. The middle step of the life cycle including translation and RNA replication was evaluated with the transient replication assay by using the HCV subgenomic replicon. Sulochrin had little effect on the replicon activity at doses up to 50 μM (Fig. 2A). In the HCVpp system, which reproduced the early step of HCV infection including entry, sulochrin significantly inhibited HCVpp infection (Fig. 2B). Sulochrin also inhibited the infection of HCVtcp, which reproduced both the viral entry and RNA replication, further supporting that this compound targeted the entry step (Fig. 2C). In contrast, VSV G-mediated viral entry efficiency was not altered by sulochrin treatment (Fig. 2D). Additionally, HBV entry was not inhibited by the presence of sulochrin (Fig. 2D). These data suggest that the inhibitory activity of sulochrin on viral entry is specific to HCV. The anti-HCV entry activity of sulochrin was conserved among different HCV genotypes, 1a (RMT), 1b (Con1), and 2a (JFH-1) [4,10,23] (Fig. 2C).

3.4. Synergistic effect of cotreatment of sulochrin with IFNα or telaprevir

We examined the anti-HCV activity of sulochrin co-administered with clinically available anti-HCV agents, IFNα and a prote-

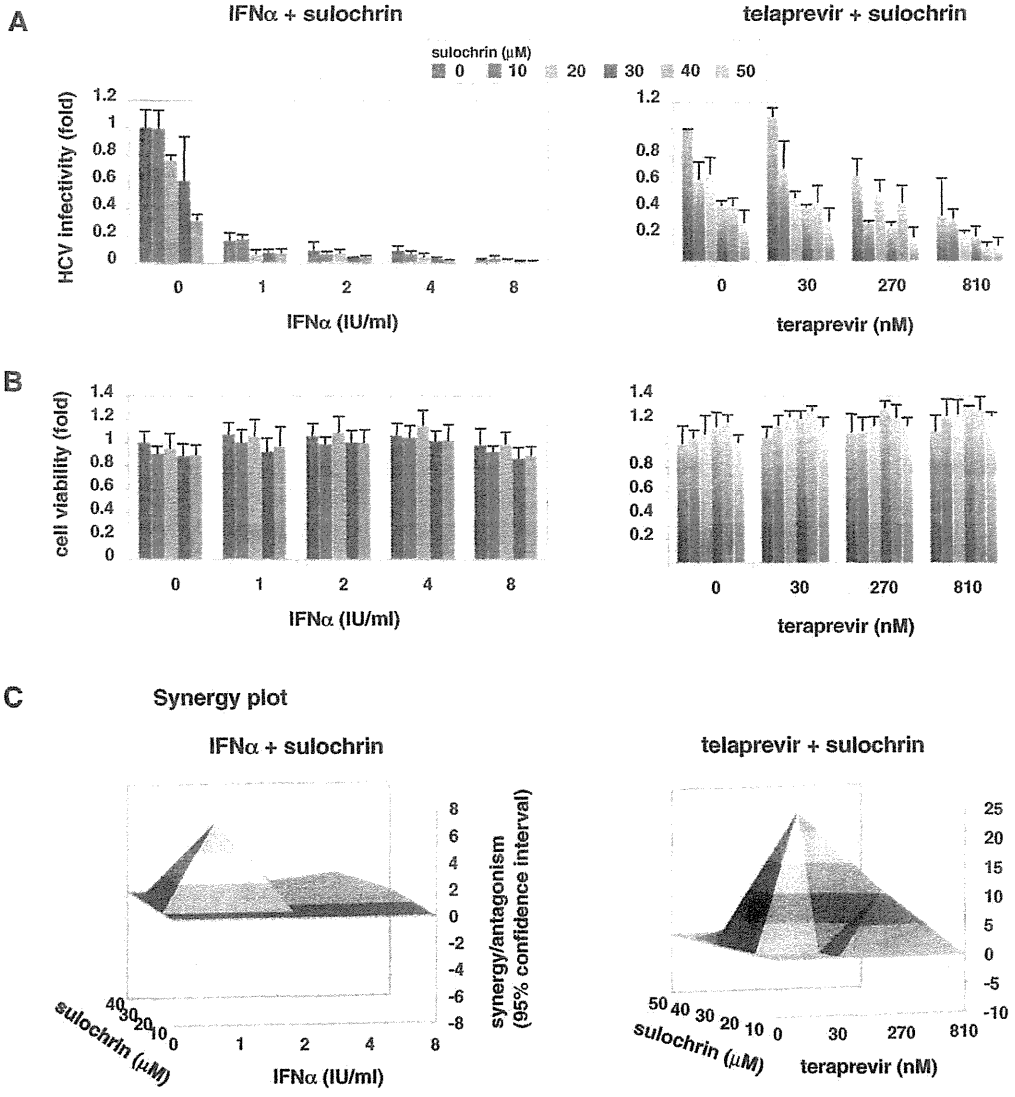

Fig. 3. Cotreatment of sulochrin with IFNα or telaprevir. (A, B) Huh-7.5.1 cells infected with HCV were treated with the indicated concentrations of sulochrin with IFNα (left) or telaprevir (right) to determine HCV infectivity in the medium (A) as shown in Fig. 1C. Cell viability was also quantified (B). (C) Synergy analysis. The results of the combinations shown in (A) were analysed with a mathematical model, MacSynergy, as described in the Section 2. The three-dimensional surface plot represents the difference between actual experimental effects and theoretical additive effects of the combination treatment (95% confidence interval). The theoretical additive effects are shown as the zero plane (dark gray) across the z-axis. A positive value in the z-axis as a peak above the plane indicates synergy, and a negative value with a valley below the plane indicates antagonism. Sulochrin in combination with IFNα (left) or telaprevir (right) produced synergistic antiviral effects that were greater than the theoretical additive effects.

ase inhibitor telaprevir. As shown in Fig. 3, addition of sulochrin with IFNα or telaprevir led to a further decrease in HCV infectivity (Fig. 3A) without significantly enhancing cytotoxicity (Fig. 3B) at any given concentrations. Thus, the combination of sulochrin and IFNα or telaprevir always resulted in a greater reduction in HCV infectivity as compared with that achieved by either agent alone. Synergy/antagonism analysis with the Bliss independence model showed that the experimental anti-HCV activity in combination with sulochrin and IFNα or telaprevir showed a peak above the zero plane in the *z*-axis, which shows the calculated theoretical additive effect (Fig. 3C). Any peak above the zero plane indicates more than an additive effect, namely, synergy (Section 2). The data clearly indicate that sulochrin had a synergistic anti-HCV effect with both IFNα and telaprevir.

3.5. Derivative analysis of sulochrin

We examined the anti-HCV activity of a series of sulochrin derivatives (Fig. 4A) in the HCVcc system. Monochlorosulochrin and dihydrogeodin, mono- or dichloro-substituted derivatives of sulochrin, possessed even higher anti-HCV activity than sulochrin (Fig. 4B and C). Deoxyfunicone, of which one aromatic ring was replaced by a 4-pyrone ring, had approximately 5-fold greater HCV inhibitory activity as compared with sulochrin (Fig. 4B and C). An additional compound, 3-*O*-methylfunicone, also possessed anti-HCV activity (Fig. 4B and C). These data suggest that the 1,3-dihydroxy-5-methylbenzene moiety of sulochrin is important for anti-HCV activity. Furthermore, funicone derivatives as well as sulochrin derivatives are likely to be lead compounds for a new class of anti-HCV agents.

4. Discussion

In the present study, we prepared a natural product library consisting of approximately 300 isolated compounds derived from fungi extract [17]. Among these compounds, we focused on sulochrin, which reduced HCV infectivity in the HCVcc system. Sulochrin suppressed the viral entry efficiencies both in the HCVpp and the HCVtcp systems, suggesting that this compound blocked HCV envelope-mediated entry. HCV was reported to enter host cells through clathrin-dependent endocytosis after engagement to host receptors [24–27]. Sulochrin is not likely to be a general inhibitor of clathrin-dependent endocytosis, but rather is specific for HCV entry, as it did not affect the entry of other viruses such as VSVpp and HBV, which were reported to enter by clathrin-dependent manners [28,29].

Sulochrin inhibits eosinophil degranulation, activation, and chemotaxis [30,31]. It also inhibits VEGF-induced tube formation of human umbilical vein endothelial cells [32]. In addition, 3-*O*-methylfunicone, a sulochrin derivative possessing anti-HCV activity, has an anti-tumor activity [33]. It is unknown if these activities of the compounds are related to their anti-HCV activity. The establishment of drug-resistant virus and the identification of the target molecule are in progress to reveal the mechanism of action of sulochrin and its derivatives. However, the present study is the

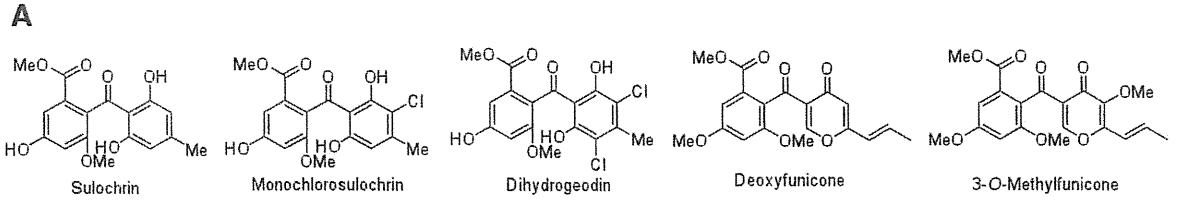

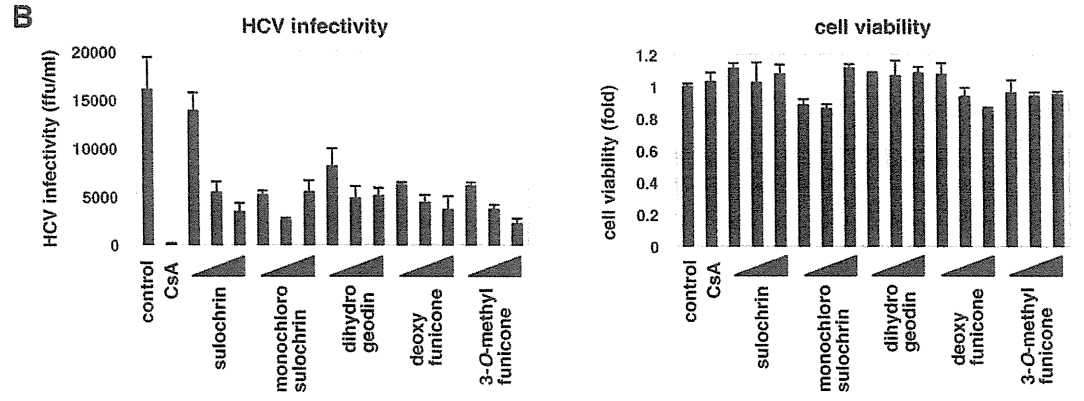

C IC_{50}s and CC_{50}s

compound	IC_{50} (μM)	CC_{50} (μM)
sulochrin	24.4 ± 2.0	> 50
monochlorosulochrin	4.3 ± 1.1	> 50
dihydrogeodin	10.3 ± 0.3	> 50
deoxyfunicone	4.6 ± 1.1	> 50
3-*O*-methylfunicone	6.2 ± 2.3	> 50

Fig. 4. Derivative analysis of sulochrin. (A) Chemical structures of sulochrin derivatives examined in this study, monochlorosulochrin, dihydrogeodin, deoxyfunicone, 3-*O*-methyfunicone, as well as sulochrin. (B) Anti-HCV effects of the sulochrin derivatives (10, 30, and 50 μM) were investigated as shown in Fig. 1C. (C) The IC_{50} and CC_{50} values of the sulochrin derivatives are shown.

first report to demonstrate the antiviral activity of these compounds. It is important to note that sulochrin inhibited the entry of HCV genotype 1a and b, which are the dominant genotypes in North America, Europe, and East Asia, indicating that this compound has potential clinical applications. Promising applications of entry inhibitors include the prevention of HCV recurrence in patients after liver transplantation. In patients with HCV-related end-stage liver diseases undergoing liver transplantation, re-infection of the graft is universal and characterised by accelerated progression of liver diseases. Entry inhibitors may be effective especially in these conditions under robust re-infection of HCV into hepatocytes. In the present study, we showed that co-treatment of sulochrin with IFNα and a protease inhibitor, teleprevir, synergistically augmented the anti-HCV effects of these approved drugs. These results suggest the possibility that co-treatment with sulochrin and probably its effective derivatives helps to inhibit the spread of HCV infection. We also identified the chemical structure and the derivatives of sulochrin as lead compounds for anti-HCV agents. Further derivatives analysis may identify more preferable anti-HCV agents.

In conclusion, our results demonstrate that sulochrin and its derivatives are potent and selective inhibitors of HCV infection in cell culture. Although further studies including an analysis of mode of action and pharmacological properties *in vivo* are required, this class of compounds should be pursued for its clinical potential in the treatment of HCV infection.

Acknowledgments

Huh-7.5.1 cells were kindly provided by Dr. Francis Chisari at The Scripps Research Institute. The expression plasmids for producing HCVpp were a generous gift from Dr. Francois-Loic Cosset at Universite de Lyon. The expression plasmid for HCV E1E2 of genotype 1a (RMT) was kindly provided by Dr. Michinori Kohara at Tokyo Metropolitan Institute of Medical Science. We thank all of the members of the Department of Virology II, National Institute of Infectious Diseases, for their helpful discussions. This study was supported by grants-in-aid from the Ministry of Health, Labour, and Welfare, Japan, from the Ministry of Education, Culture, Sports, Science, and Technology, Japan, and from the Japan Society for the Promotion of Science.

Appendix A. Supplementary data

Supplementary data associated with this article can be found, in the online version, at http://dx.doi.org/10.1016/j.bbrc.2013.09.100.

References

[1] T.J. Liang, V. Rustgi, E. Golan, H.E. Blum, HCV RNA in patients with chronic hepatitis C treated with interferon-alpha, J. Med. Virol. 40 (1993) 69–75.

[2] J.G. McHutchison, S.C. Gordon, E.R. Schiff, M.L. Shiffman, W.M. Lee, V.K. Rustgi, Z.D. Goodman, M.H. Ling, S. Cort, J.K. Albrecht, Interferon alfa-2b alone or in combination with ribavirin as initial treatment for chronic hepatitis C. Hepatitis Interventional Therapy Group, N. Engl. J. Med. 339 (1998) 1485–1492.

[3] A.W. Tai, R.T. Chung, Treatment failure in hepatitis C: mechanisms of non-response, J. Hepatol. 50 (2009) 412–420.

[4] V. Lohmann, F. Korner, J. Koch, U. Herian, L. Theilmann, R. Bartenschlager, Replication of subgenomic hepatitis C virus RNAs in a hepatoma cell line, Science 285 (1999) 110–113.

[5] B. Bartosch, J. Dubuisson, F.L. Cosset, Infectious hepatitis C virus pseudo-particles containing functional E1–E2 envelope protein complexes, J. Exp. Med. 197 (2003) 633–642.

[6] M. Hsu, J. Zhang, M. Flint, C. Logvinoff, C. Cheng-Mayer, C.M. Rice, J.A. McKeating, Hepatitis C virus glycoproteins mediate pH-dependent cell entry of pseudotyped retroviral particles, Proc. Natl. Acad. Sci. USA 100 (2003) 7271–7276.

[7] T. Wakita, T. Pietschmann, T. Kato, T. Date, M. Miyamoto, Z. Zhao, K. Murthy, A. Habermann, H.G. Krausslich, M. Mizokami, R. Bartenschlager, T.J. Liang, Production of infectious hepatitis C virus in tissue culture from a cloned viral genome, Nat. Med. 11 (2005) 791–796.

[8] J. Zhong, P. Gastaminza, G. Cheng, S. Kapadia, T. Kato, D.R. Burton, S.F. Wieland, S.L. Uprichard, F. Wakita, F.V. Chisari, Robust hepatitis C virus infection in vitro, Proc. Natl. Acad. Sci. USA 102 (2005) 9294–9299.

[9] B.D. Lindenbach, M.J. Evans, A.J. Syder, B. Wolk, T.L. Tellinghuisen, C.C. Liu, T. Maruyama, R.O. Hynes, D.R. Burton, J.A. McKeating, C.M. Rice, Complete replication of hepatitis C virus in cell culture, Science 309 (2005) 623–626.

[10] R. Suzuki, K. Sato, T. Kato, M. Shirakura, D. Akazawa, K. Ishii, H. Aizaki, Y. Kanegae, Y. Matsuura, I. Saito, T. Wakita, T. Suzuki, Trans-complemented hepatitis C virus particles as a versatile tool for study of virus assembly and infection, Virology 422 (2012) 29–38.

[11] G.M. Cragg, D.J. Newman, Natural products: a continuing source of novel drug leads, Biochim. Biophys. Acta 2013 (1830) 3670–3695.

[12] D.J. Newman, G.M. Cragg, Natural products as sources of new drugs over the 30 years from 1981 to 2010, J. Nat. Prod. 75 (2012) 311–335.

[13] A.L. Harvey, Natural products as a screening resource, Curr. Opin. Chem. Biol. 11 (2007) 480–484.

[14] S.X. Yang, G.M. Cragg, D.J. Newman, J.H. Buder, Natural product-based anti-HIV drug discovery and development facilitated by the NCI developmental therapeutics program, J. Nat. Prod. 69 (2006) 488–498.

[15] K. Iwatsuki, Y. Wang, N. Kobayashi, Viral infectious disease and natural products with antiviral activity, Drug Discovery Ther. 1 (2007) 14–22.

[16] K. Watashi, G. Liang, M. Iwamoto, H. Marusawa, N. Uchida, T. Daito, K. Kitamura, M. Muramatsu, H. Ohashi, T. Kiyohara, R. Suzuki, J. Li, S. Tong, Y. Tanaka, K. Murata, H. Aizaki, T. Wakita, Interleukin-1 and tumor necrosis factor-alpha trigger restriction of hepatitis B virus infection via a cytidine deaminase AID, J. Biol Chem. PMID: 24025329.

[17] Y. Myohatake, T. Takeuchi, K. Kuramochi, T. Kuriyama, T. Ishido, K. Hirano, F. Sugawara, H. Yoshida, Y. Mizushina, Pinophilins A and B, inhibitors of mammalian A-, B- and Y-family DNA polymerases and human cancer cell proliferation, J. Nat. Prod. 75 (2012) 135–141.

[18] A. Murayama, N. Sugiyama, K. Watashi, T. Masaki, R. Suzuki, H. Aizaki, T. Mizuochi, T. Wakita, T. Kato, Japanese reference panel of blood specimens for evaluation of hepatitis C virus RNA and core antigen quantitative assays, J. Clin. Microbiol. 50 (2012) 1943–1949.

[19] K. Watashi, M. Khan, V.R. Yedavalli, M.L. Yeung, E. Strebel, K.T. Jeang, Human immunodeficiency virus type 1 replication and regulation of APOBEC3G by peptidyl prolyl isomerase Pin1, J. Virol. 82 (2008) 9629–9636.

[20] K. Watashi, M.L. Yeung, M.F. Starost, K.S. Hosmane, K.T. Jeang, Identification of small molecules that suppress microRNA function and reverse tumorigenesis, J. Biol. Chem. 285 (2010) 24707–24716.

[21] T. Kato, T. Date, M. Miyamoto, M. Sugiyama, Y. Tanaka, E. Orito, T. Ohno, K. Sugihara, I. Hasegawa, K. Fujiwara, K. Ito, A. Ozasa, M. Mizokami, T. Wakita, Detection of anti-hepatitis C virus effects of interferon and ribavirin by a sensitive replicon system, J. Clin. Microbiol. 43 (2005) 5679–5684.

[22] H. Marusawa, M. Hijikata, K. Watashi, T. Chiba, K. Shimotohno, Regulation of Fas-mediated apoptosis by NF-kappa B activity in human hepatocyte-derived cell lines, Microbiol. Immunol. 45 (2001) 485–489.

[23] I. Yasui, M. Sudoh, M. Arai, M. Kohara, Synthetic lipophilic antioxidant ONO-853 suppresses HCV replication, J. Med. Virol. 85 (2013) 241–249.

[24] M.B. Zeisel, L. Fofana, S. Fafi-Kremer, T.F. Baumert, Hepatitis C virus entry into hepatocytes: molecular mechanisms and targets for antiviral therapy, J. Hepatol. 54 (2011) 566–576.

[25] E. Blanchard, S. Belouzard, L. Goueslain, T. Wakita, J. Dubuisson, C. Wychowski, Y. Rouille, Hepatitis C virus entry depends on clathrin-mediated endocytosis, J. Virol. 80 (2006) 6964–6972.

[26] A. Codran, C. Royer, D. Jaeck, M. Bastien-Valle, T.F. Baumert, M.P. Kieny, C.A. Pereira, J.P. Martin, Entry of hepatitis C virus pseudotypes into primary human hepatocytes by clathrin-dependent endocytosis, J. Gen. Virol. 87 (2006) 2583–2593.

[27] L. Meertens, C. Bertaux, T. Dragic, Hepatitis C virus entry requires a critical postinternalisation step and delivery to early endosomes via clathrin-coated vesicles, J. Virol. 80 (2006) 11571–11578.

[28] D.K. Cureton, R.H. Massol, S.P. Whelan, T. Kirchhausen, The length of vesicular stomatitis virus particles dictates a need for actin assembly during clathrin-dependent endocytosis, PLoS Pathog. 6 (2010) e1001127.

[29] H.C. Huang, C.C. Chen, W.C. Chang, M.H. Tao, C. Huang, Entry of hepatitis E virus into immortalized human primary hepatocytes by clathrin-dependent endocytosis, J. Virol. 86 (2012) 9443–9453.

[30] H. Ohashi, M. Ishikawa, J. Ito, A. Ueno, G.J. Gleich, H. Kita, H. Kawai, H. Fukamachi, Sulochrin inhibits eosinophil degranulation, J. Antibiotechnol. (Tokyo) 50 (1997) 972–974.

[31] H. Ohashi, Y. Motegi, H. Kita, G.J. Gleich, T. Miura, M. Ishikawa, H. Kawai, H. Fukamachi, Sulochrin inhibits eosinophil activation and chemotaxis, Inflamm. Res. 47 (1998) 409–415.

[32] H.J. Lee, J.H. Lee, B.Y. Hwang, H.S. Kim, J.J. Lee, Fungal metabolites, asterric acid derivatives inhibit vascular endothelial growth factor (VEGF)-induced tube formation of HUVECs, J. Antibiotechnol. (Tokyo) 55 (2002) 552–556.

[33] R. Nicoletti, E. Manzo, M.L. Ciavatta, Occurrence and bioactivities of fusicoccin-related compounds, Int. J. Mol. Sci. 10 (2009) 1430–1444.

Signal Peptidase Complex Subunit 1 Participates in the Assembly of Hepatitis C Virus through an Interaction with E2 and NS2

Ryosuke Suzuki[1]*, Mami Matsuda[1], Koichi Watashi[1], Hideki Aizaki[1], Yoshiharu Matsuura[2], Takaji Wakita[1], Tetsuro Suzuki[3]*

1 Department of Virology II, National Institute of Infectious Diseases, Tokyo, Japan, 2 Research Institute for Microbial Diseases, Osaka University, Osaka, Japan, 3 Department of Infectious Diseases, Hamamatsu University School of Medicine, Shizuoka, Japan

Abstract

Hepatitis C virus (HCV) nonstructural protein 2 (NS2) is a hydrophobic, transmembrane protein that is required not only for NS2-NS3 cleavage, but also for infectious virus production. To identify cellular factors that interact with NS2 and are important for HCV propagation, we screened a human liver cDNA library by split-ubiquitin membrane yeast two-hybrid assay using full-length NS2 as a bait, and identified signal peptidase complex subunit 1 (SPCS1), which is a component of the microsomal signal peptidase complex. Silencing of endogenous SPCS1 resulted in markedly reduced production of infectious HCV, whereas neither processing of structural proteins, cell entry, RNA replication, nor release of virus from the cells was impaired. Propagation of Japanese encephalitis virus was not affected by knockdown of SPCS1, suggesting that SPCS1 does not widely modulate the viral lifecycles of the *Flaviviridae* family. SPCS1 was found to interact with both NS2 and E2. A complex of NS2, E2, and SPCS1 was formed in cells as demonstrated by co-immunoprecipitation assays. Knockdown of SPCS1 impaired interaction of NS2 with E2. Our findings suggest that SPCS1 plays a key role in the formation of the membrane-associated NS2-E2 complex via its interaction with NS2 and E2, which leads to a coordinating interaction between the structural and non-structural proteins and facilitates the early step of assembly of infectious particles.

Citation: Suzuki R, Matsuda M, Watashi K, Aizaki H, Matsuura Y, et al. (2013) Signal Peptidase Complex Subunit 1 Participates in the Assembly of Hepatitis C Virus through an Interaction with E2 and NS2. PLoS Pathog 9(8): e1003589. doi:10.1371/journal.ppat.1003589

Editor: Aleem Siddiqui, University of California, San Diego, United States of America

Received February 1, 2013; **Accepted** July 19, 2013; **Published** August 29, 2013

Funding: This work was supported by a grant-in-aid for Scientific Research from the Japan Society for the Promotion of Science, from the Ministry of Health, Labour and Welfare of Japan and from the Ministry of Education, Culture, Sports, Science and Technology of Japan. The funders had no role in study design, data collection and analysis, decision to publish, or preparation of the manuscript.

Competing Interests: The authors have declared that no competing interests exist.

* E-mail: ryosuke@nih.go.jp (RS); tesuzuki@hama-med.ac.jp (TS)

Introduction

Over 170 million people worldwide are chronically-infected with hepatitis C virus (HCV), and are at risk of developing chronic hepatitis, cirrhosis, and hepatocellular carcinoma [1]. HCV is an enveloped virus of the family *Flaviviridae*, and its genome is an uncapped 9.6-kb positive-strand RNA consisting of the 5′ untranslated region (UTR), an open reading frame encoding viral proteins, and the 3′ UTR [2]. A precursor polyprotein is further processed into structural proteins (Core, E1, and E2), followed by p7 and nonstructural (NS) proteins (NS2, NS3, NS4A, NS4B, NS5A, and NS5B), by cellular and viral proteases. The structural proteins (Core to E2) and p7 reside in the N-terminal region, and are processed by signal peptidase from the polyprotein. NS2, NS3, and NS4A are prerequisites for proteolytic processing of the NS proteins. NS3 to NS5B are considered to assemble into a membrane-associated HCV RNA replicase complex. NS3 also possesses activities of helicase and nucleotide triphosphatase. NS4 is a cofactor that activates the NS3 protease. NS4B induces vesicular membrane alteration. NS5A is considered to play an important but undefined role in viral RNA replication. NS5B is the RNA-dependent RNA polymerase. It is now accepted that NS proteins, such as NS2, NS3, and NS5A, contribute to the assembly or release of infectious HCV [3–9].

NS2 protein is a transmembrane protein of 21–23 kDa, with highly hydrophobic N-terminal residues forming transmembrane helices that insert into the endoplasmic reticulum (ER) membrane [5,10]. The C-terminal part of NS2 resides in the cytoplasm, enabling zinc-stimulated NS2/3 autoprotease activity together with the N-terminal domain of NS3. The crystal structure of the C-terminal region of NS2 reveals a dimeric cysteine protease containing two composite active sites [11]. Prior work showed that NS2 is not essential for RNA replication of subgenomic replicons [12]; however, the protein is required for virus assembly independently of protease activity [5,6]. Several adaptive mutations in NS2 that increase virus production have been reported [13–17]. In addition, there is increasing evidence for genetic and biochemical interaction of NS2 with other HCV proteins, including E1, E2, p7, NS3-4A, and NS5A [10,18–25]. Thus, NS2 is now suggested to act as a scaffold to coordinate interactions between the structural and NS proteins for viral assembly. However, the molecular mechanism by which NS2 is involved in virus assembly remains unclear.

In this study, we identified signal peptidase complex subunit 1 (SPCS1) as a host factor that interacts with NS2 by yeast two-hybrid screening with a split-ubiquitin system. SPCS1 is a component of the microsomal signal peptidase complex which is

Author Summary

Viruses hijack host cells and utilize host-derived proteins for viral propagation. In the case of hepatitis C virus (HCV), many host factors have been identified that are required for genome replication; however, only a little is known about cellular proteins that interact with HCV proteins and are important for the viral assembly process. The C-terminal half of nonstructural protein 2 (NS2), and the N-terminal third of NS3, form the NS2-3 protease that cleaves the NS2/3 junction. NS2 also plays a key role in the viral assembly process independently of the protease activity. We performed split-ubiquitin yeast two-hybrid screening and identified signal peptidase complex subunit 1 (SPCS1), which is a subunit of the microsomal signal peptidase complex. In this study, we provide evidence that SPCS1 interacts with both NS2 and E2, resulting in E2-SPCS1-NS2 complex formation, and has a critical role in the assembly of infectious HCV particles. To our knowledge, SPCS1 is the first NS2-interacting cellular factor that is involved in regulation of the HCV lifecycle.

responsible for the cleavage of signal peptides of many secreted or membrane-associated proteins. We show that SPCS1 is a novel host factor that participates in the assembly process of HCV through an interaction with NS2 and E2.

Results

SPCS1 is a novel host protein that interacts with HCV NS2 protein

To gain a better understanding of the functional role of NS2 in the HCV lifecycle, we screened a human liver cDNA library by employing a split-ubiquitin membrane yeast two-hybrid system with the use of NS2 as a bait. It is known that the split ubiquitin-based two-hybrid system makes it possible to study protein-protein interactions between integral membrane proteins at the natural sites of interactions in cells [26]. From the screening, several positive clones were identified from the 13 million transformants, and the nucleotide sequences of the clones were determined. A BLAST search revealed that one of the positive clones encodes a full-length coding region of signal peptidase complex subunit 1 (SPCS1). SPCS1 is a component of the microsomal signal peptidase complex which consists of five different subunit proteins in mammalian cells [27]. Although catalytic activity for SPCS1 has not been indicated to date, a yeast homolog of this subunit is involved in efficient membrane protein processing as a component of the signal peptidase complex [28].

To determine the specific interaction of NS2 with SPCS1 in mammalian cells, FLAG-tagged NS2 (FLAG-NS2; Fig. 1A) was co-expressed in 293T cells with myc-tagged SPCS1 (SPCS1-myc; Fig. 1A), followed by co-immunoprecipitation and immunoblotting. SPCS1 was shown to be co-immunoprecipitated with NS2 (Fig. 1B). Co-immunoprecipitation of SPCS1-myc with NS2 was also observed in the lysate of Huh-7 cells infected with cell culture-produced HCV (HCVcc) derived from JFH-1 isolate [29] (Fig. 1C). To determine the region of SPCS1 responsible for the interaction with NS2, deletion mutants of myc-tagged SPCS1 were constructed (Fig. 1A) and co-expressed with FLAG-tagged NS2. Since the expression of C-terminal deletion mutants, d3 and d4, was difficult to detect (Fig. 1D), N-terminal deletions (d1 and d2) as well as wild-type SPCS1 were subjected to immunoprecipitation analysis. SPCS1-myc, -d1, and -d2 were co-immunoprecipitated with NS2 (Fig. 1E), suggesting that the SPCS1 region spanning amino acids (aa) 43 to 102 is involved in its interaction with NS2. Next, to identify the NS2 region responsible for its interaction with SPCS1, deletion mutants for FLAG-NS2 (Fig. 1A) were co-expressed with SPCS1-myc-d2 in cells, followed by being immunoprecipitated with anti-myc antibody. SPCS1 was co-immunoprecipitated with the NS2 deletions, except for a mutant lacking transmembrane (TM) 2 and TM3 (dTM23) domains (Fig. 1F). These finding suggests that the TM3 region of NS2 is involved in the interaction with SPCS1.

To investigate SPCS1-NS2 interaction *in situ*, the proximity ligation assay (PLA) [30], which is based on antibodies tagged with circular DNA probes, was used. Only when the antibodies are in close proximity, the probes can be ligated together and subsequently be amplified with a polymerase. We were able to detect PLA signal predominantly in the cytoplasm of the cells expressing FLAG-NS2 and SPCS1-myc-d2 tagged with V5 at N-terminus (Fig. 1G). By contrast, the PLA signal was not observed in the context of NS2-Core co-expression. We further analyzed the SPCS1-NS2 interaction by the monomeric Kusabira-Green (mKG) system [31], which is based on fusion proteins with complementary fragments (mKG-N and mKG-C) of the monomeric coral fluorescent reporter protein. When the mKG fragments are in close proximity due to the protein-protein interaction, the mKG fragments form a beta-barrel structure and emit green fluorescence. Co-expression of SPCS1-mKG-N and NS2-mKG-C fusion proteins in cells reconstituted green cellular fluorescence as shown in Fig. 1H. Thus, these results represented structures with SPCS1 and NS2 in close proximity, and strongly suggest their physical interaction in cells.

SPCS1 participates in the propagation of infectious HCV particles

To investigate the role(s) of endogenous SPCS1 in the propagation of HCV, four small interfering RNAs (siRNAs) for SPCS1 with different target sequences or scrambled control siRNA were transfected into Huh7.5.1 cells, followed by infection with HCVcc. Among the four SPCS1-siRNAs, the highest knockdown level was observed by siRNA #2. siRNAs #3 and #4 showed moderate reductions of SPCS1 expression, and only a marginal effect was obtained from siRNA #1 (Fig. 2A). As indicated in Fig. 2B, the infectious viral titer in the culture supernatant was significantly reduced by the knockdown of SPCS1. It should be noted that the infectious titers correlated well with the expression levels of endogenous SPCS1. siRNA #2 reduced the HCV titer to ~5% of the control level in Huh7.5.1 cells. To rule out the possibility of off-target effect of SPCS1-siRNA on HCV propagation, we also used "C911" mismatch control siRNAs in which bases 9 through 11 of siRNAs are replaced with their complements but other parts of antisense- and sense-strand sequences are kept intact. These mismatch designed-control siRNAs have been shown to reduce the down-regulation of the targeted mRNA, but maintains the off-target effects of the original siRNA [32]. The C911 controls against SPCS1-siRNA #2, #3, and #4 (C911-#2, -#3, and -#4) showed little effect on knockdown of SPCS1 as well as propagation of HCV (Fig. S1A and B).

We further determined the loss- and gain-of-function of SPCS1 on HCV propagation in an SPCS1-knockdown cell line. To this end, Huh-7 cells were transfected with a plasmid encoding a short hairpin RNA (shRNA) targeted to SPCS1 and were selected with hygromycin B, resulting in clone KD#31 where little or no expression of SPCS1 was detectable (Fig. 2C). KD#31 cells and parental Huh-7 cells were transfected with an RNA polymerase I (pol)-driven full-genome HCV plasmid [33] in the presence or

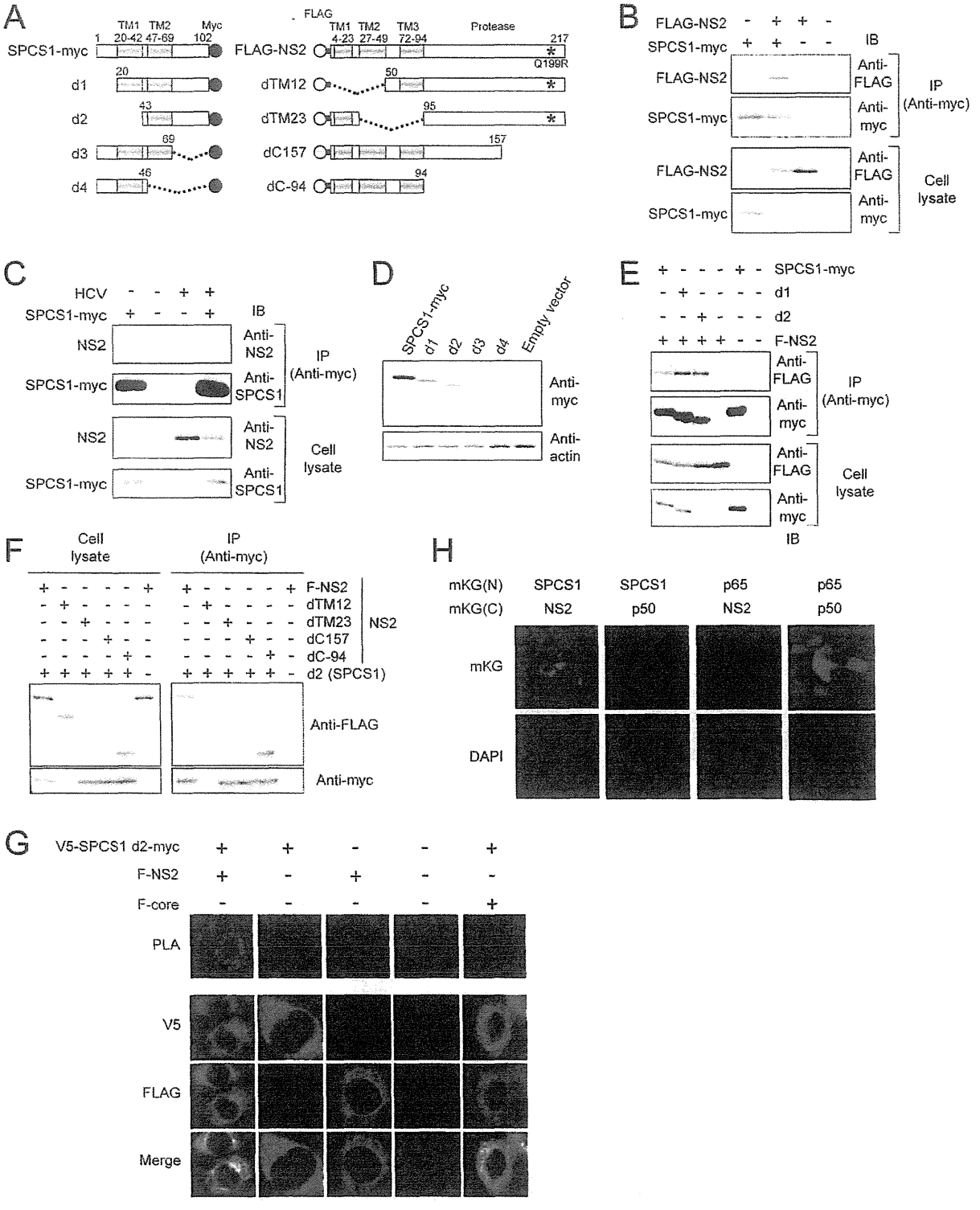

Figure 1. Interaction of HCV NS2 protein with SPCS1 in mammalian cells. (A) Expression constructs of SPCS1-myc and FLAG-NS2 used in this study. TM regions are represented as gray. Myc-tag regions are depicted by the black circles. Gray circles and bold lines indicated FLAG-tag and spacer (GGGGS) sequences, respectively. Adaptive mutations are indicated as asterisks. Positions of the aa resides are indicated above the boxes. (B) 293T cells were co-transfected with a FLAG-tagged NS2 expression plasmid in the presence of a SPCS1-myc expression plasmid. Cell lysates of the transfected cells were immunoprecipitated with anti-myc antibody. The resulting precipitates and whole cell lysates used in immunoprecipitation (IP) were examined by immunoblotting using anti-FLAG- or anti-myc antibody. An empty plasmid was used as a negative control. (C) HCVcc infected

Huh-7 cells were transfected with a SPCS1-myc expression plasmid. Cell lysates of the transfected cells were immunoprecipitated with anti-myc antibody. The resulting precipitates and whole cell lysates used in immunoprecipitation (IP) were examined by immunoblotting using anti-NS2 or anti-SPCS1 antibody. (D) Expression of SPCS1-myc and its deletion mutants. 293T cells were transfected with indicated plasmids. The cell lysates were examined by immunoblotting using anti-myc or anti-actin antibody. (E) Cells were co-transfected with indicated plasmids, and then lysates of transfected cells were immunoprecipitated with anti-myc antibody. The resulting precipitates and whole cell lysates used in IP were examined by immunoblotting using anti-FLAG- or anti-myc antibody. (F) Lysates of the transfected cells were immunoprecipitated with anti-myc antibody. The resulting precipitates (right panel) and whole cell lysates used in IP (left panel) were examined by immunoblotting using anti-FLAG or anti-myc antibody. (G) 293T cells were transfected with indicated plasmids. 2 days posttransfection, cells were fixed and permeabilized with Triton X-100, then subjected to in situ PLA (Upper) or immunofluorescence staining (Lower) using anti-FLAG and anti-V5 antibodies. (H) Detection of the SPCS1-NS2 interaction in transfected cells using the mKG system. 293T cells were transfected by indicated pair of mKG fusion constructs. Twenty-four hours after transfection, cell were fixed and stained with DAPI, and observed under a confocal microscope.
doi:10.1371/journal.ppat.1003589.g001

absence of an expression plasmid for shRNA-resistant SPCS1 (SPCS1- sh^r). Western blotting confirmed the expression levels of SPCS1 in cells (Fig. 2D). As expected, viral production in the culture supernatants of the transfected cells was significantly impaired in SPCS1-knockdown cells compared with parental Huh-7 cells (Fig. 2E white bars). Expression of SPCS1- sh^r in KD#31 cells recovered virus production in the supernatant to a level similar to that in the parental cells. Expression of SPCS1-sh^r in parental Huh-7 cells did not significantly enhance virus production. Taken together, these results demonstrate that SPCS1 has an important role in HCV propagation, and that the endogenous expression level of SPCS1 is sufficient for the efficient propagation of HCV.

A typical feature of the *Flaviviridae* family is that their precursor polyprotein is processed into individual mature proteins mediated by host ER-resident peptidase(s) and viral-encoded protease(s). We therefore next examined the role of SPCS1 in the propagation of Japanese encephalitis virus (JEV), another member of the *Flaviviridae* family. SPCS1 siRNAs or control siRNA were transfected into Huh7.5.1 cells followed by infection with JEV or HCVcc. Although knockdown of SPCS1 severely impaired HCV production (Fig. 3A), the propagation of JEV was not affected under the SPCS1-knockdown condition (Fig. 3B). Expression of the viral proteins as well as knockdown of SPCS1 were confirmed (Fig. 3C). This suggests that SPCS1 is not a broadly active modulator of the flavivirus lifecycle, but rather is involved specifically in the production of certain virus(es) such as HCV.

Knockdown of SPCS1 exhibits no influence on the processing of HCV proteins and the secretion of host-cell proteins

Since SPCS1 is a component of the signal peptidase complex, which plays a role in proteolytic processing of membrane proteins at the ER, it may be that SPCS1 is involved in processing HCV

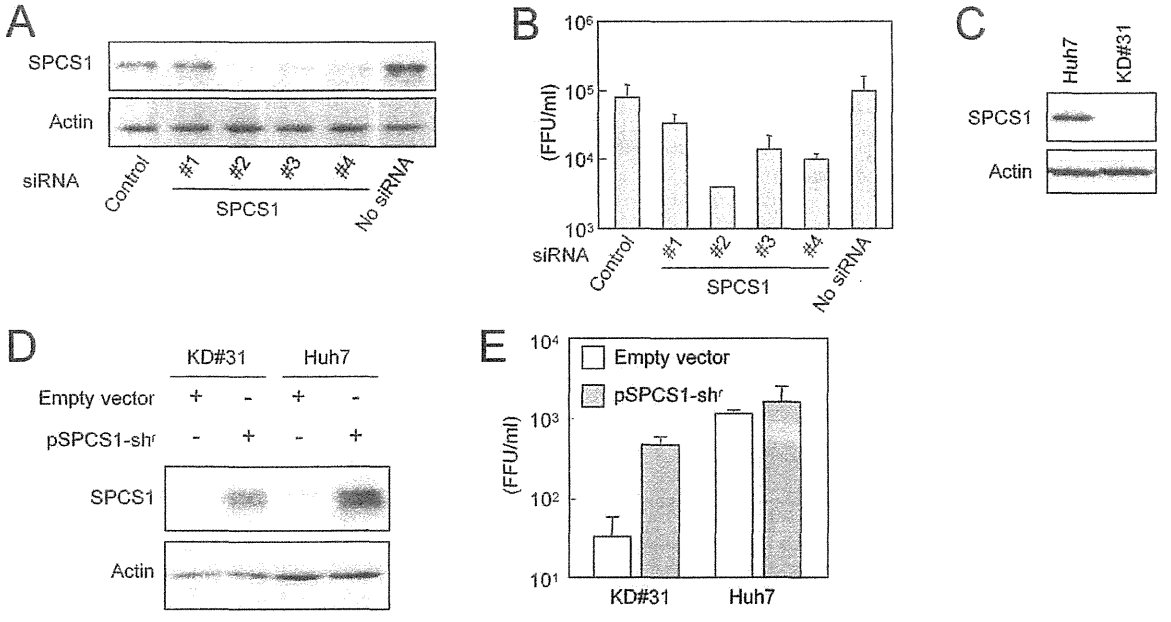

Figure 2. Effect of SPCS1 knockdown on the production of HCV. (A) Huh7.5.1 cells were transfected with four different siRNAs targeted for SPCS1 or control siRNA at a final concentration of 15 nM, and infected with HCVcc at a multiplicity of infection (MOI) of 0.05 at 24 h post-transfection. Expression levels of endogenous SPCS1 and actin in the cells were examined by immunoblotting using anti-SPCS1 and anti-actin antibodies at 3 days post-infection. (B) Infectious titers of HCVcc in the supernatant of cells infected as above were determined at 3 days postinfection. (C) Huh-7 cells were transfected with pSilencer-SPCS1, and hygromycin B-resistant cells were selected. The SPCS1-knockdown cell line established (KD#31) and parental Huh-7 cells were subjected to immunoblotting to confirm SPCS1 knockdown. (D) KD#31 cells or parental Huh-7 cells were transfected with RNA pol I-driven full-length HCV plasmid in the presence or absence of shRNA-resistant SPCS1 expression plasmid. Expression levels of SPCS1 and actin in the cells at 5 days post-transfection were examined by immunoblotting using anti-SPCS1 and anti-actin antibodies. (E) Infectious titers of HCVcc in the supernatants of transfected SPCS1-knockdown cells or parental Huh-7 cells at 5 days post-transfection were determined.
doi:10.1371/journal.ppat.1003589.g002

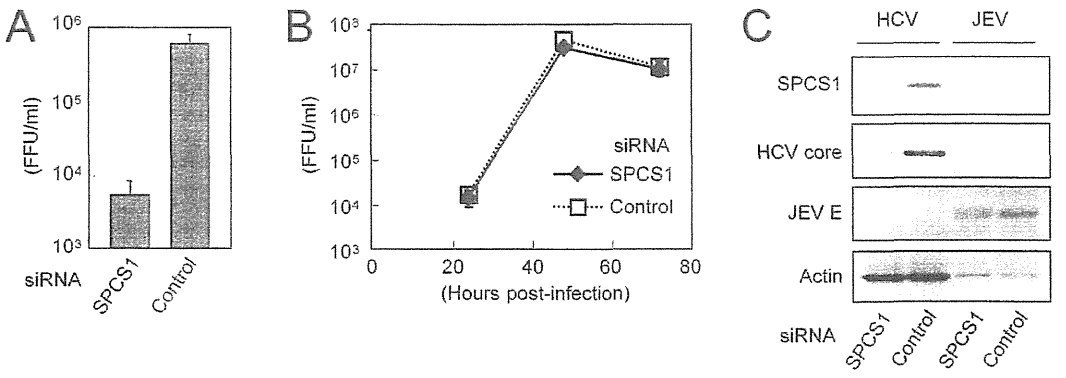

Figure 3. Effect of SPCS1 knockdown on the propagation of JEV. Huh7.5.1 cells were transfected with SPCS1 siRNA or control siRNA at a final concentration of 10 nM, and infected with JEV or HCVcc at an MOI of 0.05 at 24 h post-transfection. (A) Infectious titers of HCVcc in the supernatant at 3 days post-infection were determined. (B) Infectious titers of JEV in the supernatant at indicated time points were determined. (C) Expression levels of endogenous SPCS1 and actin as well as viral proteins in the cells were determined by immunoblotting using anti-SPCS1, anti-actin, anti-HCV core, and anti-JEV antibodies 3 days post-infection.
doi:10.1371/journal.ppat.1003589.g003

proteins via interacting with ER membranes. To address this, the effect of SPCS1 knockdown on the processing of HCV precursor polyproteins in cells transiently expressing the viral Core-NS2 region was analyzed. Western blotting indicated that properly processed core and NS2 were observed in KD#31 cells as well as Huh-7 cells (Fig. 4A). No band corresponding to the unprocessed precursor polyprotein was detected in either cell line (data not shown). We also examined the effect of SPCS1 knockdown on the cleavage of the NS2/3 junction mediated by NS2/3 protease. Processed NS2 was detected in both cell lines with and without SPCS1 knockdown, which were transfected with wild-type or protease-deficient NS2-3 expression plasmids (Fig. 4B & C).

Signal peptidase plays a key role in the initial step of the protein secretion pathway by removing the signal peptide and releasing the substrate protein from the ER membrane. It is now accepted that the secretion pathways of very-low density lipoprotein or apolipoprotein E (apoE) are involved in the formation of infectious HCV particles and their release from cells [34,35]. ApoE is synthesized as a pre-apoE. After cleavage of its signal peptide in the ER, the protein is trafficked to the Golgi and trans-Golgi network before being transported to the plasma membrane and secreted. As shown in Fig. 4D, the secreted levels of apoE from Huh-7 cells with knocked-down of SPCS1 were comparable to those from control cells. In addition, the level of albumin, an abundant secreted protein from hepatocytes, in the culture supernatants of the cells was not influenced by SPCS1 knockdown (Fig. 4E). These data suggest that the knockdown of SPCS1 has no influence on the processing of viral and host secretory proteins by signal peptidase and HCV NS2/3 protease.

SPCS1 is involved in the assembly process of HCV particles but not in viral entry into cells and RNA replication

To further address the molecular mechanism(s) of the HCV lifecycle mediated by SPCS1, we examined the effect of SPCS1 knockdown on viral entry and genome replication using single-round infectious trans-complemented HCV particles (HCVtcp) [33], of which the packaged genome is a subgenomic replicon containing a luciferase reporter gene. This assay system allows us to evaluate viral entry and replication without the influence of reinfection. Despite efficient knockdown of SPCS1 (Fig. 5A), luciferase activity expressed from HCVtcp in SPCS1-knockdown cells was comparable to that in control or non-siRNA-transfected cells (Fig. 5B), suggesting that SPCS1 is not involved in viral entry into cells and subgenomic RNA replication. As a positive control, knockdown of claudin-1, a cell surface protein required for HCV entry, reduced the luciferase activity. We also examined the effect of SPCS1 knockdown on full-genome replication using HCVcc-infected cells. Despite efficient knockdown of SPCS1, expression of HCV proteins was comparable to that in control cells (Fig. 5C). By contrast, knockdown of PI4 Kinase (PI4K), which is required for replication of HCV genome, led to decrease in expression of HCV proteins. As cells that had already been infected with HCV were used, knockdown of claudin-1 had no effect on HCV protein levels. These data suggest that SPCS1 is not involved in viral entry into cells and the viral genome replication. We also observed properly processed Core, E2, NS2 and NS5B in SPCS1-knockdown cells in consistent with the result as shown in Fig. 4A, indicating no effect of SPCS1 on HCV polyprotein processing.

Next, to investigate whether SPCS1 is involved in the assembly or release of infectious particles, SPCS1-shRNA plasmid along with a pol I-driven full-genome HCV plasmid [33] were transfected into CD81-negative Huh7-25 cells, which can produce infectious HCV upon introduction of the viral genome, but are not permissive to HCV infection [36]. It is therefore possible to examine viral assembly and the release process without viral reinfection. The infectivity within the transfected cells as well as supernatants was determined 5 days post-transfection. Interestingly, both intra- and extracellular viral titers were markedly reduced by SPCS1 knockdown (Fig. 5C).

Taken together, in the HCV lifecycle, SPCS1 is most likely involved in the assembly of infectious particles rather than cell entry, RNA replication, or release from cells.

Role of SPCS1 in complex formation between NS2 and E2

It has been shown that HCV NS2 interacts with the viral structural and NS proteins in virus-producing cells [18–21], and that some of the interactions, especially the NS2-E2 interaction, are important for the assembly of infectious HCV particles. However, the functional role of NS2 in the HCV assembly process has not been fully elucidated. To test whether SPCS1 is involved in the interaction between NS2 and E2, cells were co-transfected

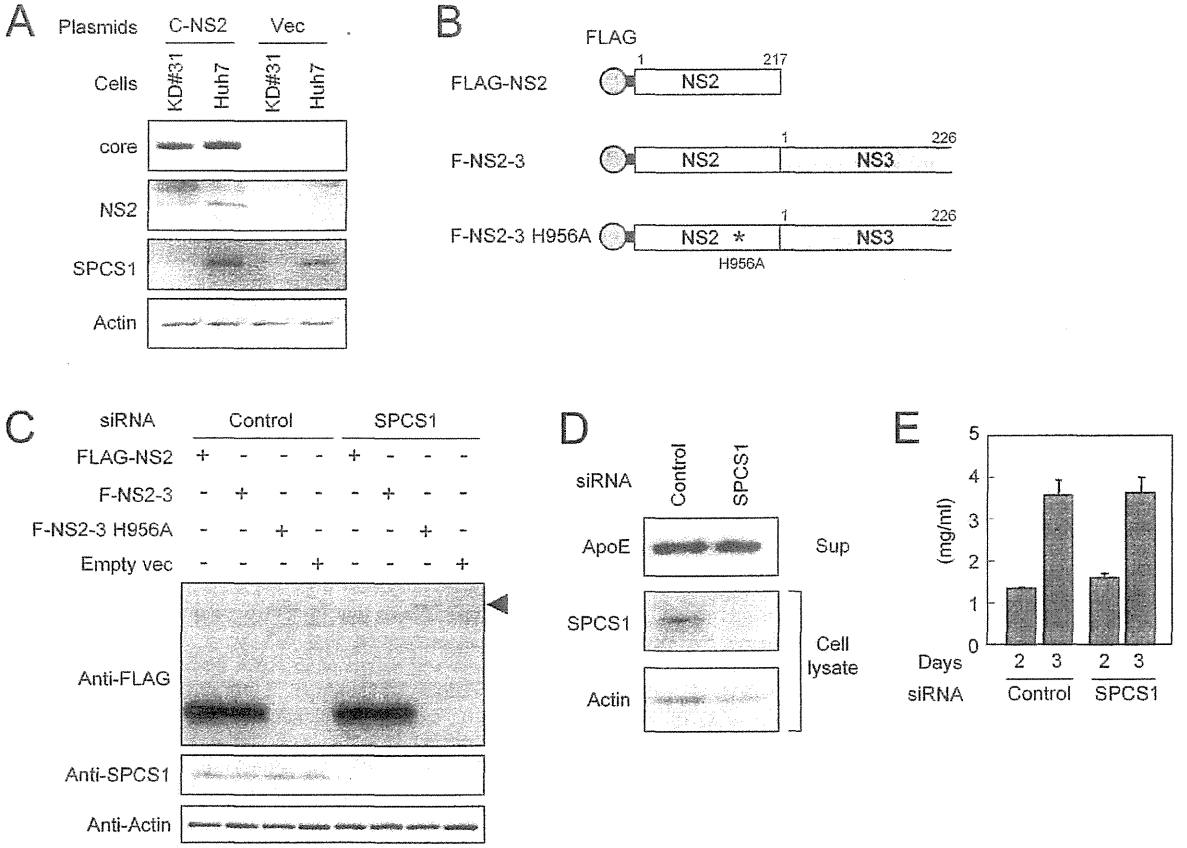

Figure 4. Effect of SPCS1 knockdown on the processing of HCV structural proteins and secretion of host proteins. (A) Core-NS2 polyprotein was expressed in KD#31 cells or parental Huh-7 cells. Core, NS2, SPCS1, and actin were detected by immunoblotting 2 days post-transfection. (B) Expression constructs of NS2 and NS2/3 proteins. His to Ala substitution mutation at aa 956 in NS2 is indicated by an asterisk. Gray circles and bold lines indicate FLAG-tag and the spacer sequences, respectively. Positions of the aa residues are indicated above the boxes. (C) Effect of SPCS1 knockdown on processing at the NS2/3 junction. Huh-7 cells were transfected with SPCS1 siRNA or control siRNA at a final concentration of 30 nM, and then transfected with plasmids for FLAG-NS2, F-NS2-3, or F-NS2-3 with a protease-inactive mutation (H956A). NS2 in cell lysates was detected by anti-FLAG antibody 2 days post-transfection. Arrowhead indicates unprocessed NS2-3 polyproteins. (D) Effect of SPCS1 knockdown on the secretion of apoE. Huh7.5.1 cells were transfected with SPCS1 siRNAs or control siRNA at a final concentration of 20 nM, and apoE in the supernatant and SPCS1 and actin in the cells were detected 3 days post-transfection. (E) Effect of SPCS1 knockdown on the secretion of albumin. Huh7.5.1 cells were transfected with SPCS1 siRNA or control siRNA, and albumin in the culture supernatants at 2 and 3 days post-transfection was measured by ELISA.
doi:10.1371/journal.ppat.1003589.g004

with expression plasmids for E2, FLAG-NS2, and SPCS1-myc. E2 and NS2 were co-immunoprecipitated with SPCS1-myc, and E2 and SPCS1-myc were co-immunoprecipitated with FLAG-NS2 (Fig. 6A), suggesting the formation of an E2-NS2-SPCS1 complex in cells. To investigate the interaction of SPCS1 with E2 in the absence of NS2, HCV Core-p7 polyprotein or E2 protein were co-expressed with SPCS1-myc in cells, followed by immunoprecipitation with anti-myc antibody. As shown in Fig. 6B and Fig. S2, E2 was co-immunoprecipitated with SPCS1-myc. The interaction between SPCS1 and E2 was further analyzed *in situ* by PLA and mKG system. Specific signals indicating formation of the SPCS1-E2 complex were detected in both assays (Fig. S3), suggesting physical interaction between SPCS1 and E2 in cells.

We further determined the region of SPCS1 responsible for the interaction with E2 by co-immunoprecipitation assays. Full-length and deletion mutant d2 of SPCS1 (Fig. 1A) were similarly co-immunoprecipitated with E2, while only a limited amount of d1 mutant SPCS1 (Fig. 1A) was co-precipitated (Fig. 6C). It may be that the aa 43–102 region of SPCS1, which was identified as the region involved in the NS2 interaction (Fig. 1D), is important for its interaction with E2, and that deletion of the N-terminal cytoplasmic region leads to misfolding of the protein and subsequent inaccessibility to E2.

Finally, to understand the significance of SPCS1 in the NS2-E2 interaction, Huh7.5.1 cells with or without SPCS1 knockdown by siRNA were transfected with expression plasmids for Core-p7 and FLAG-NS2, followed by co-immunoprecipitation with anti-FLAG antibody. As shown in Fig. 6D, the NS2-E2 interaction was considerably impaired in the SPCS1-knockdown cells as compared to that in the control cells. A similar result was obtained in the stable SPCS1-knockdown cell line (Fig. 6E). In contrast, in that cell line, the interaction of NS2 with NS3 was not impaired by SPCS1 knockdown (Fig. 6E).

These results, together with the above findings, suggest that SPCS1 is required for or facilitates the formation of the membrane-associated NS2-E2 complex, which participates in the proper assembly of infectious particles.

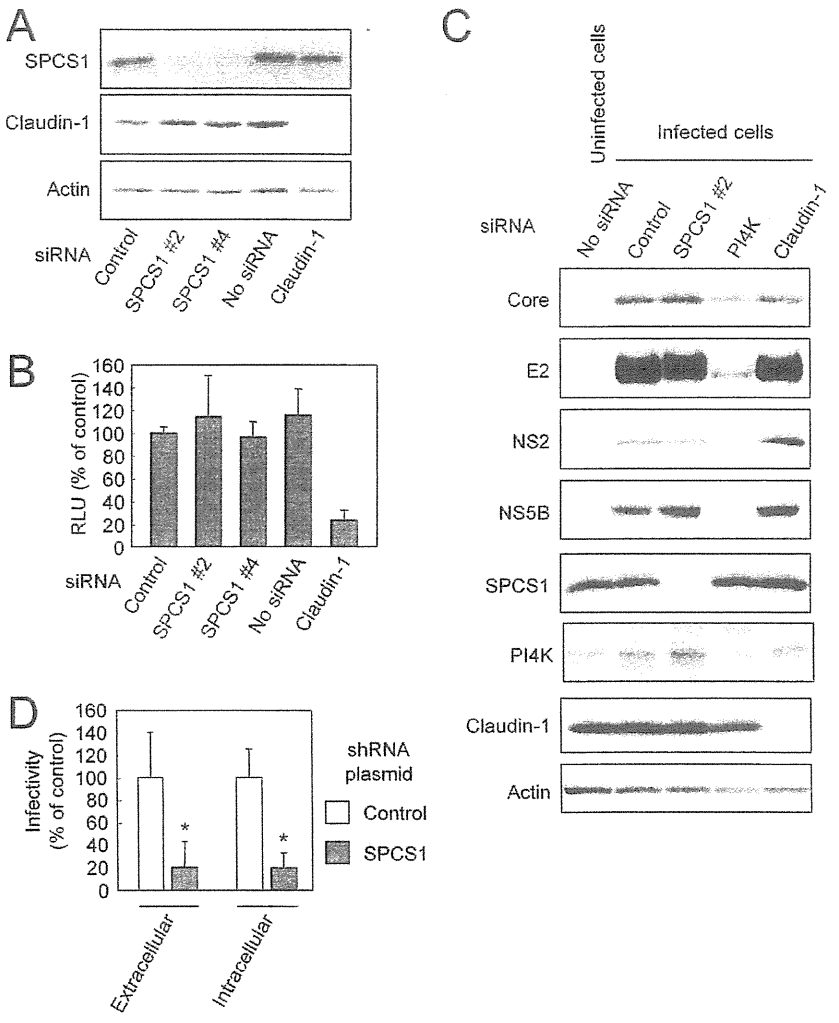

Figure 5. Effect of SPCS1 knockdown on entry into cells, genome replication, and assembly or release of infectious virus. (A) Huh7.5.1 cells were transfected with siRNA for SPCS1 or claudin1, or control siRNA at a final concentration of 30 nM. Expression levels of endogenous SPCS1, claudin-1, and actin in the cells at 2 days post-transfection were examined by immunoblotting using anti-SPCS1, anti-actin, and anti-claudin-1 antibodies. (B) Huh7.5.1 cells transfected with indicated siRNAs were infected with HCVtcp at 2 days post-transfection. Luciferase activity in the cells was subsequently determined at 2 days post-infection. Data are averages of triplicate values with error bars showing standard deviations. (C) Effect of SPCS1 knockdown on replication of HCV genome. HCV-infected Huh-7 cells transfected with siRNA for SPCS1, PI4K or claudin1, or control siRNA at a final concentration of 30 nM. Expression levels of HCV proteins as well as endogenous SPCS1, PI4K, claudin-1, and actin in the cells at 3 days post-transfection were examined by immunoblotting. (D) HCV infectivity in Huh7.5.1 cells inoculated with culture supernatant and cell lysate from Huh7-25 cells transfected with pSilencer-SPCS1 or control vector along with pHH/JFH1am at 5 days post-transfection. Statistical differences between Control and SPCS1 knockdown were evaluated using Student's t-test. *$p<0.005$ vs. Control.
doi:10.1371/journal.ppat.1003589.g005

Discussion

In this study, we identified SPCS1 as a novel host factor that interacts with HCV NS2, and showed that SPCS1 participates in HCV assembly through complex formation with NS2 and E2. In general, viruses require host cell-derived factors for proceeding and regulating each step in their lifecycle. Although a number of host factors involved in genome replication and cell entry of HCV have been reported, only a few for viral assembly have been identified to date. To our knowledge, this is the first study to identify an NS2-interacting host protein that plays a role in the production of infectious HCV particles.

NS2 is a hydrophobic protein containing TM segments in the N-terminal region. The C-terminal half of NS2 and the N-terminal third of NS3 form the protease, which is a prerequisite for NS2-NS3 cleavage. In addition, it is now accepted that this protein is essential for particle production [4-6,12]. However, the mechanism of how NS2 is involved in the assembly process of HCV has been unclear.

So far, two studies have screened for HCV NS2 binding proteins by yeast two-hybrid analysis [37,38]. Erdtmann et al. reported that no specific interaction was detected by a conventional yeast hybrid screening system using full-length NS2 as a bait, probably due to hampered translocation of the bait to the